Electrical Power and Energy Systems 102 (2018) 131–151

Contents lists available at ScienceDirect

Electrical Power and Energy Systems

journal homepage: www.elsevier.com/locate/ijepes

Accentuating the renewable energy exploitation: Evaluation of flexibility options

Juan Manuel Alemany[a,b,c,d,*], Bartlomiej Arendarski[a], Pio Lombardi[a], Przemyslaw Komarnicki[a]

[a] IFF Fraunhofer, Magdeburg, Germany
[b] Otto von Guericke Universität, Magdeburg, Germany
[c] Universidad Nacional de Rio Cuarto, Argentina
[d] CONICET, Argentina

ARTICLE INFO

Keywords:
Demand response
Energy storage systems
Horizontal energy transactions
Mixed Integer Linear Programming
Power grid flexibility
Renewables integration

ABSTRACT

A global energy transition is currently happening mainly through the shift from conventional to renewable electricity resources in power energy systems. On this transition, the flexibility of the power grid complies a fundamental role to permit the full integration of renewables. Therefore, the purpose of this work is to develop a methodology that permits evaluating the current technological flexibility options available in power grids to exploit the integration of renewables fully. A Mixed Integer Linear Programming model is developed. The model incorporates pumped energy and battery storage systems, demand response, virtual power plant, and transmission-distribution energy transactions. The work is focused on the operation planning considering daily, weekly and seasonal factors regarding renewables and load patterns. The general results show, that all the flexibility options have the capacity to integrate, in a mayor extent, the renewable energy into the power grid. For example, from a base integration of 40.6% of renewable energy, all the flexi-options added an extra 27.1% of energy from RES. Suggesting, that the best option to integrate renewables is the incorporation of a diverse set of flexibility options. Interestingly, options like demand response and virtual power plant, presented the best renewables integration figures (17.9% and 6.9%) compared to options like energy storages (6.05% average). Therefore, it is strongly recommendable to analyze particularly options which, with plausible modifications and minor investment requirements, can offer a suitable flexibility capacity to the existent power grid. Finally, distribution-distribution or transmission-distribution energy transactions also have a great potential to diminish the renewable curtailment. For example, they permitted integrating an extra 13.9% and 93.53% respectively, for the full flexi-option.

1. Introduction

The large scale integration of Renewable Energy Sources (RES), like wind and photovoltaic generation, presents a significant challenge to any power system due to the uncertainty of these resources. Normally, this is the first mentioned drawback about the exploitation of RES. However, it is rarely mentioned that RES, especially wind generation, possess a high and fast change rate of active power injection to the grid [1], added up to a frequency response that depends on power electronics rather than inertial physics. These two factors are critical in stability matter because the network has been designed to work with relatively small or slow, power change rates and to count on large amounts of energy stored in the inertia of large generators. Consequently, large and sudden power flow variations in the network produce a numerous quantity of undesirable effects. Therefore, it is important to evaluate different strategies-that subsequently evolve in new methodologies-that allow a secure and efficient operation of the power system under high penetration of RES. In this sense, the flexibility of the power grid complies a fundamental role to permit the full integration of RES.

1.1. Motivation

This work is mainly motivated by the current German energy scenario; nevertheless, this study represents no impediment to be considered as a comparative model for other power systems confronting currently, or in the future, the same energy transition challenge.

Germany has designed an energy transition to trigger a change in the energy system and technologies. Mainly through the shift from conventional to renewable energy. This transition pursue for smart

* Corresponding author at: IFF Fraunhofer, Magdeburg, Germany.
E-mail address: jalemany@ing.unrc.edu.ar (J.M. Alemany).

https://doi.org/10.1016/j.ijepes.2018.04.023
Received 23 October 2017; Received in revised form 7 April 2018; Accepted 19 April 2018

energy use and better consumer participation coupled with the implementation of energy efficiency measures. The German transition is a long-term and evolving process. This concept adopted in 2010, have resulted in a considerable RES deployment in Germany, particularly in the power sector. For example, more than 19% of the countrys electricity generation was from RES in the year 2010. Currently, nearly 34% (>185 TWh) of the total generation is from RES [2]. Now is entering the next phase of this transition, focused on how higher shares of RES can be accommodated and how the grid infrastructure can be expanded to ensure that the power system and its actors are more flexible to allow for the integration of electricity from RES.

In 2016, the share of RES wind and solar in power generation exceeded 21.2% [3]. This share was achieved without any major problems. Factors contributing to this achievement include the strength of the German grid, flexibility of conventional generation, balancing markets, forecasting, trades with neighboring countries and improvements in distribution systems. The successes achieved thus far, are not sufficient to take Germanys RES share to 35% of the total energy mix by the countrys 2020 target [4]. Higher shares of RES will require more flexibility and balancing. To trace the way for higher shares of RES, an active discussion around two competitive market designs a capacity market and an energy-only market is on the run. Also, flexibility for renewable grid integration is under discussion; ranging from cross-border and neighboring grids exchange and expansion to demand-side management and storage [5] with various technologies for each voltage level.

Given this energy transition scenario, this work is focused on the evaluation of the most prominent flexibility options available nowadays in the German power grids.

1.2. Approach

This work is focused on the operation planning without disregarding daily, weekly and seasonal factors which strongly affect RES and load patterns. In this sense, we define monthly scheduling horizons for the summer, winter and autumn seasons. These seasons are commonly considered the most representatives to enrich a realistic study with the incorporation of weather effects.

This work evaluates different flexibility options, existent or to be incorporated. This aim is achieved analyzing the behavior of variables such as generation costs, RES generation and spillage, reserve contributions, and energy transactions with the Transmission System Operator (TSO) and with neighboring Distribution System Operator (DSO).

A Mixed Integer Linear Programming (MILP) model is developed. Different flexibility options are considered, for example, Pumped Energy Storage System (PESS), Battery Energy Storage Systems (BESS), Industrial Demand Responses (DR), and Vertical-Horizontal Energy Interchanges. The emphasis is placed in the maximum exploitation of renewable energy with the minimum impact on higher voltage levels of the grid.

We use a Germany's regional grid with yearly demand, wind and solar patterns. Representative scenarios, monthly-seasonal patterns, are simulated. Simulation steps of 15 min are used to capture the sudden changes of RES. A linear AC network formulation is derived under properly given assumptions. This approach has proven to be accurate enough for the purpose of this work.

1.3. Literature review

To the best of our knowledge, we were unable to find a similar work to ours. That is to say, reference works (to compare) proposing a model to numerically evaluate the integration of RES into grids incorporating different flexibility options. In this sense, we collected works focused in: the integration of RES to the grid; with any flexibility option among the ones we incorporate in our model; and the evaluation of RES potential into real power systems. Most of the works found are real case evaluations and very recent, thus, they form a starting point to consider the current importance of the topic by the research community. In this regard, articles [6–9] deserve to be highlighted as very detailed and exhaustive reviews.

Studies which incorporate a storage flexibility option are: work [14] which analyzes the Portugals energy system planning for achieving 100% RES electricity production; work [22] which considers the impact of integrating RES with EVs; work [24] which assesses the wind market value in Sweden where hydroelectric stations with large reservoirs prevail; work [25] which analyzes how RES and storage systems can contribute to improve the energy independence and reliability of isolated power systems located in remote areas of Russia; work [26] which uses a multi-period equilibrium model to simulate power markets incorporating different types of generators and energy storage systems; and work [13] which explores a storage market for RES grid integration with a production cost model.

Regarding the BESS option, work [12] focuses on the operation, size and cycling of a Li-ion-based BESS to limit the variability of photovoltaic power plants. Additionally, work [27] shows a BESS new business model by offering flexibility to system operators. Regarding the PESS option, work [15] analyzes different scenarios of increased penetration of RES in Cape Verde's power system, using pumped hydro as a storage technique.

Demand response applications are vastly, to our work's aim can be mentioned: work [17] which analyzes the DR potential across all the European demand sectors like industrial and residential ones; work [18] which compares different strategies for fixed and flexible loads in the dispatch optimization of an isolated system; work [19] which focuses on a more accurate representation of the Irish power sector, integrating operational constraints associated to the short-term horizon while maintaining the temporal resolution of long-term model; and work [20] which presents a method for generation system planning, specifically accounting for flexibility at high penetration levels of RES.

Regarding grid interconnections, work [21] focuses on the potential of coordination among TSOs with respect to operation of controllable devices like phase-shifting transformers and high-voltage direct current.

Several works gather mixed flexibility options, among them we can cite: work [16] which examines the replacement of conventional energy sources by RES under storage and interconnection; work [23] which explores flexibility options for high levels of RES integration and reliability in France; work [11] which evaluates the integration of high shares of RES with PESS, BESS, EV and European grid interconnections in the long-term evolution of the power system; and work [10] which proposes a cost optimization planning model of the USA electricity system, evaluating flexibility mechanisms like storage and DR from EVs.

1.4. Contributions

Considering the above literature review, the contributions of this study are:

1. To develop a methodology that permits evaluating the current technological flexibility options available in power grids to exploit the integration of RES fully. The model incorporates pumped energy and battery storage systems, demand response, virtual power plant, and TSO-DSO/DSO-DSO energy transactions.
2. To develop a methodology to evaluate the potential of horizontal energy transactions between DSO.
3. To carry out a number of insightful, realistic studies to comprehend the effects of using these options and to measuring up to which extent RES can be exploited.
4. To derive some recommendations to facilitate the process of the energy transition from a thermal-dominated to a renewable-dominated electric power system.

1.5. Organization

The paper is organized as follows. Section 2, describes the general planning model of this work. In Section 3, a detailed description of the network modeling is given. Section 4, enumerates all the flexibility option models included in this work. Section 5, details the experimental settings. Section 6, presents the numerical results and the corresponding discussion. Finally, Section 7 summarizes the main conclusions of this work.

2. Methodology

To evaluate the maximum integration of energy injected from RES into the power grid, we formulate an optimization problem for the operation planning of all the elements that participate such as generation, storage, and demand resources. We propose to solve this problem for a medium-term scheduling horizon with time steps of fifteen minutes. We assume that a time step of this order permits to capture the variability of the wind and solar patterns accurately. Besides, we assume that a medium-term horizon permits to capture weekly and seasonal components on the patterns. In this regard, we present the objective function and the set of constraints that conform the optimization problem. Moreover, we present the particular formulation for each of the generation resources and flexibility options available on the grid. Please note that the formulations are developed under the per unit system.

2.1. Nomenclature

Acronyms

BESS	Battery Energy Storage System
DR	Demand Response
DSO	Distribution System Operator
EV	Electric Vehicle
LHS, RHS	left/right hand side
OF	objective function
PESS	Pumped Energy Storage System
RES	renewable energy sources
TSO	transmission system operator
VPP	virtual power plant
wi,*pv*	wind, photovoltaic
bi,*co*	biomass, conventional
vpp	virtual power plant
vi,*hi*	vertical/horizontal interchanges
ba	battery energy storage system
ge,*pu*	and generation/pumping modes

Sets

t	index for time steps
T	time steps set
b,i,j	indexes for buses
B,$\overline{\text{J}}$	bus sets
g	index for generators
G	generators set
k	DR blocks
K	total DR blocks
B^{wi}	buses with wind farms
B^{pv}	buses with pv farms
B^{vpp}	buses with VPP
B^{vi}	buses with vi
β	index for piecewise approximation
G^{res}	units that participate on reserve
B^{vres}	TSO buses participating on reserve.
B^{dem}	buses with demand
τ	start-up steps

Variables

TC,PC_{gt},SC_{gt}	total/production/start-up costs
p_{bt},q_{bt}	active and reactive injections
$p^{co}_{g\in b,t}$	conventional active power
$q^{co}_{g\in b,t}$	conventional reactive power.
p^{wi}_{bt}	wind farm active power
p^{pv}_{bt}	pv farm active power
p^{bi}_{gt}	biomass plant active power
p^{vi}_{bt}	MW from/to *vi*
p^{hi}_{bt}	MW from/to *hi*
p^{ba}_{bt}	BESS active power
q^{bi}_{gt}	biomass plant reactive power
q^{wi}_{bt}	wind farm reactive power
q^{pv}_{bt}	pv farm reactive power
q^{ge}_{bt}	PESS gen mode reactive power
q^{vi}_{bt}	MVAr from/to vertical interchange
dr_{tk},dr_{bt}	DR variable for each block or bus
u_{gt},s_{gt},h_{gt}	status/start-up/shut-down states
$\delta_{\beta gt}$	PC piecewise power variable
re_{gt},vre_{bt}	reserve variables
ΔVI_{ω}	*vi* piecewise power variable
p^{vi}_{ω}	*vi* piecewise power limits
P_i,Q_i	active/reactive bus balances
$\lvert V_b\rvert$,θ_b	voltage magnitude and phase
V^{Pen},B^{Pen}_{soc},VI^{Pen}	penalization terms
p^{ge}_{bt},p^{pu}_{bt}	PESS gen/pump mode powers
u^{ge}_{bt},u^{pu}_{bt}	and statuses
P^{soc}_{bt},B^{soc}_{bt}	PESS and BESS state of charges
p^{vpp}_{bt},d^{vpp}_{bt}	VPP generation/demand services
ug^{vpp}_{bt},ud^{vpp}_{bt}	and statuses
$pf_{i,j,t}$,$qf_{i,j,t}$	active/reactive power flows

Parameters

λ_t,λ_t^+,λ_t^-	price signals
be_k	DR utility value
π	penalization weights
$\text{Tr}_{\beta g}$	PC piecewise power limits
c_g	PC min cost value
$\text{F}_{\beta g}$	PC piecewise slopes
$\underline{\text{P}}_g$,$\overline{\text{P}}_g$,$\underline{\text{Q}}_g$,$\overline{\text{Q}}_g$,$\overline{\text{P}}_b$	min/max power limits
$\text{K}_{g\tau}$	start-up coefficients
RU_g,RD_g	ramping limits
Patt^{wi}_t,Patt^{su}_t,Patt^{vpp}_t	wind/sun/VPP patterns
$\underline{\text{VI}}_b$,$\overline{\text{VI}}_b$	*vi* power limits
d^{ac}_{bt},d^{re}_{bt}	active/reactive demands
R	reserve requirement
G_{ij},B_{ij}	conductance/susceptance matrices
γ	branch susceptances matrix
S^{prime}	branch-bus incidence matrix
b^{shunt}_i,$\text{b}^{branch}_{i,j}$	branch parameters
$\lvert\overline{\text{S}_{i,j}}\rvert$,$\lvert\text{S}_{pu}\rvert$	MVA flow limit and pu value
ρ_{ω}	penalty values for each point ω
ω_n	points for the piecewise function

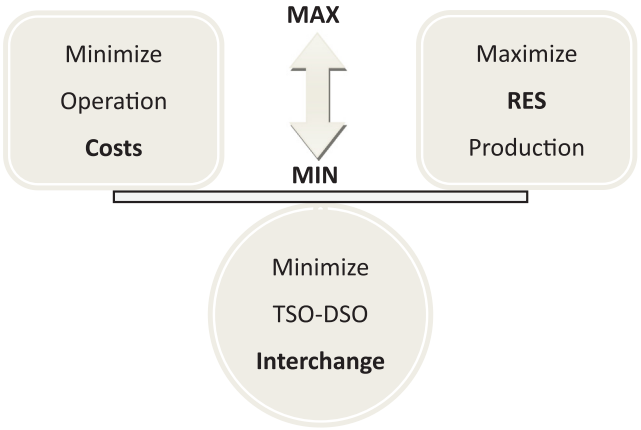

Fig. 1. Objective Functions Balance.

α_ω	slopes of the piecewise segments
ΔV_ω	voltage magnitude ω range
$\underline{eV}$,$\overline{eV}$	min/max emergency voltages
$\underline{V}$,$\overline{V}$	min/max normal voltages
$\overline{\mathrm{PG}}$,$\overline{\mathrm{PP}}$,$\overline{\mathrm{BP}}$	gen/pump and BESS power rates
η	PESS/BESS efficiencies
P_0^{soc}	PESS initial state of charge
$\underline{\mathrm{PE}}$,$\overline{\mathrm{PE}}$,$\underline{\mathrm{BE}}$,$\overline{\mathrm{BE}}$	PESS/BESS energy limits
ΔB_ω^{soc}	BESS state of charge ω range
$\overline{\mathrm{DR}}^h$	max DR during a single period
$\underline{\mathrm{VPP}}$,$\overline{\mathrm{VPP}}$	VPP min/max power limits.

2.2. Objective function

Three specific objectives were proposed to be pursued in this work. Fig. 1 shows a representative schema of them. Hierarchically stated, these objectives are:

1. Maximization of Renewable Energy Generation.
2. Minimization of Total Operation Costs.
3. Minimization of Vertical Energy Interchange.

Under this scheme, the different objective functions (OF) could be interpreted as a multiple objective optimization problem [28]. However, the main feature of such problems is the competitive nature of the different objectives. A deeper analysis of Fig. 1 offers a better insight into how these objectives relate each other. For example, if the aim were to maximize RES generation, then the natural result would be a decrease of the total operation costs which mainly depend on fuel costs. Thus, the objectives are not competing, in fact, they are negative correlated. Also, the vertical energy interchange can be considered as a part of the second objective when energy is purchased from higher levels, and part of the first objective when energy is sold to higher levels. Hence, the aim of this work is to couple this three objectives on a unique and general OF.

Mathematically, the objective function, Eq. (1), is constituted by four terms. The first term represents the RES, wind and solar, generation. The second term represents the operational costs related to the conventional generation and the demand response. The third term represents the virtual power plant transactions. The fourth term represents the penalizations which further explanation is given in subsequent sections. Interchange of energy between the TSO and the DSO is included in the fourth term.

$$\begin{aligned}\min TC=&\\ &-\sum_{t>1}^{\mathrm{T}}\sum_{b\in\{\mathrm{B}^{wi},\mathrm{B}^{pv}\}}(p_{bt}^{wi}+p_{bt}^{pv})\\ &+\sum_{t>1}^{\mathrm{T}}\left\{\sum_{g=1}^{\mathrm{G}^{co}}(PC_{gt}+SC_{gt})+\sum_{k=1}^{\mathrm{K}}(\lambda_t-be_k)dr_{tk}\right\}\\ &+\sum_{t>1}^{\mathrm{T}}\sum_{b\in\{\mathrm{B}^{vpp}\}}(\lambda_t^{+}\,p_{bt}^{vpp}+\lambda_t^{-}\,d_{bt}^{vpp})\\ &+\pi\sum_{t>1}^{\mathrm{T}}\sum_{b\in\{\mathrm{B}^{vi}_{,}\}}(V^{Pen}+B_{soc}^{Pen}+VI^{Pen})\end{aligned}\tag{1}$$

2.3. Conventional generation units

In a power grid highly integrated with RES, conventional generation is necessary. It is also useful to have strong links with neighbor grids or higher voltage levels. Conventional generation technologies possess the mechanical inertia and controllability to keep the sudden changes of RES within safe operation ranges. Besides, they can contribute significantly to the reactive power demands of the grid.

In this work, we take into account the main characteristics of conventional generation modeling. For example, production and start-up costs and technical constraints like ramp and power limits. Constraints like minimum service times are not modeled because they are not binding in the specific cases studied.

Biomass generation can be strictly considered as RES, however, due to their stiff and not random energy production, we considered this technology as must-run units. Also, they can be modeled with production and start-up functions and we included them in the conventional generation set. These units do not have frequent cycling states like start-up/shut-down processes. They neither have ramp limits because the range between power limits is limited during generation.

2.3.1. Unit production costs

Production costs are modeled like a convex linear piecewise approximation [29]. Eqs. (2)–(7) model the production costs which are represented in Fig. 2.

$$PC_{gt}=u_{gt}\,\mathrm{c}_g+\sum_{\beta}\mathrm{F}_{\beta g}\,\delta_{\beta gt}\quad\forall\,gt\tag{2}$$

$$p_{gt}^{co}=u_{gt}\,\underline{\mathrm{P}}_g+\sum_{\beta}\delta_{\beta gt}\quad\forall\,gt\tag{3}$$

$$\delta_{1gt}\leqslant \mathrm{Tr}_{1g}-\underline{\mathrm{P}}_g\quad\forall\,gt\tag{4}$$

$$\delta_{\beta gt}\leqslant \mathrm{Tr}_{\beta g}-\mathrm{Tr}_{\beta-1,g}\quad\forall\,gt\beta\in\{2\ldots\overline{\beta}-1\}\tag{5}$$

$$\delta_{Bgt}\leqslant \overline{\mathrm{P}}_g-\mathrm{Tr}_{B-1,g}\quad\forall\,gt\tag{6}$$

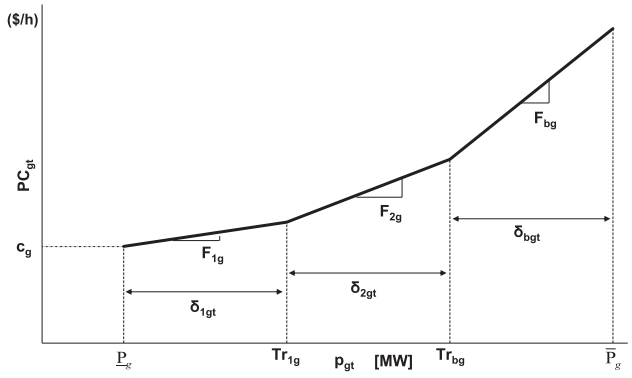

Fig. 2. Convex Production Costs for Conventional Units.

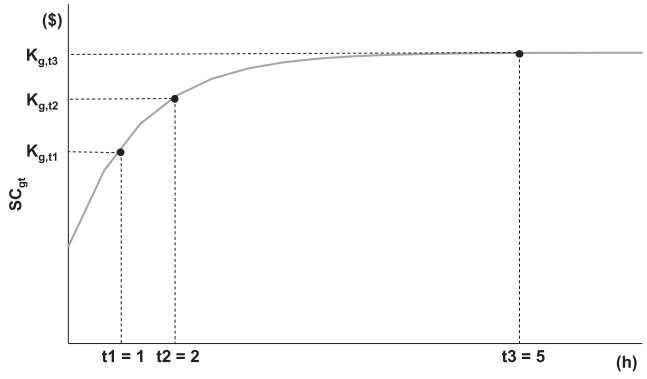

Fig. 3. Start-Up Costs for Conventional Units.

$$\delta_{\beta gt} \geqslant 0 \quad \forall\, \beta gt \tag{7}$$

$$u_{gt} \in \{0,1\} \quad \forall\, t > 1 \tag{8}$$

2.3.2. Unit start-up costs

Start-up costs are modeled with a time-dependent stepwise approximation [30]. Hot, warm and cold states can be considered. Eqs. (9) and (10) model the start-up costs which are represented in Fig. 3.

$$SC_{gt} \geqslant \mathrm{K}_{gr}\left(u_{gt} - \sum_{n=1}^{\tau} u_{g,t-n}\right) \quad \forall\, gt \tag{9}$$

$$0 \leqslant SC_{gt} \leqslant \max_{\tau}\{\mathrm{K}_{gr}\} \quad \forall\, \mathrm{gt} \tag{10}$$

2.3.3. Unit power limits

A generator model based on rectangle constraints is considered [29]. Generator capabilities are modeled with independent maximum and minimum limits on active and reactive power outputs. Eqs. (11)–(15) model the unit power limits which are represented in Fig. 4.

$$p_{gt}^{co} + re_{gt} \leqslant u_{gt}\, \overline{\mathrm{P}}_g \quad \forall\, t > 1, g \in \mathrm{G}^{co} \tag{11}$$

$$p_{gt}^{co} \geqslant u_{gt}\, \underline{\mathrm{P}}_g \quad \forall\, t > 1, g \in \mathrm{G}^{co} \tag{12}$$

$$u_{gt}\, \underline{\mathrm{P}}_g \leqslant p_{gt}^{bi} \leqslant u_{gt}\, \overline{\mathrm{P}}_g \quad \forall\, t > 1, g \in \mathrm{G}^{bi} \tag{13}$$

$$u_{gt}\, \underline{\mathrm{Q}}_g \leqslant q_{gt}^{co} \leqslant u_{gt}\, \overline{\mathrm{Q}}_g \quad \forall\, t > 1, g \in \mathrm{G}^{co} \tag{14}$$

$$u_{gt}\, \underline{\mathrm{Q}}_g \leqslant q_{gt}^{bi} \leqslant u_{gt}\, \overline{\mathrm{Q}}_g \quad \forall\, t > 1, g \in \mathrm{G}^{bi} \tag{15}$$

2.3.4. Unit ramp limits

The start-up and shut-down processes are considered within the ramp limits [29]. Eqs. (16) and (17) model the unit ramp limits. Fig. 5 illustrates the ramp limits.

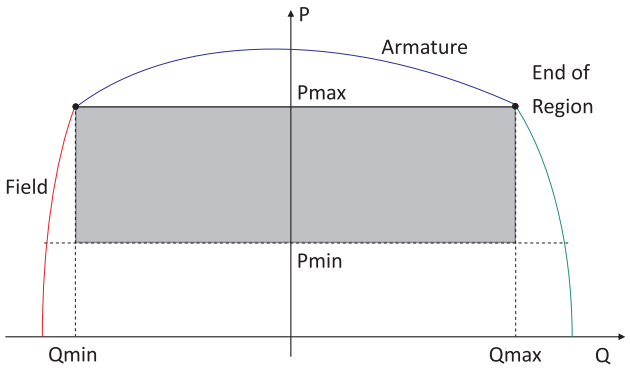

Fig. 4. Rectangular Power Limits.

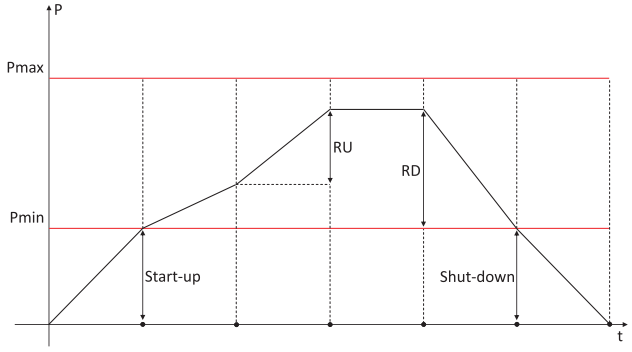

Fig. 5. Ramp limits.

$$p_{gt} - p_{g,t-1} \leqslant \mathrm{RU}_g + s_{gt}\, \underline{\mathrm{P}}_g \quad \forall\, g, t > 1 \tag{16}$$

$$p_{g,t-1} - p_{gt} \leqslant \mathrm{RD}_g + h_{gt}\, \underline{\mathrm{P}}_g \quad \forall\, g, t > 1 \tag{17}$$

$$s_{gt}, h_{gt} \in \{0,1\} \quad \forall\, t > 1 \tag{18}$$

2.4. Renewable generation resources

Individual wind turbines or photovoltaic panels are not modeled as unitary entities. Instead, they are aggregated as clusters, i.e., wind or solar farms.

2.4.1. Operational costs

the main component of cost in the operation horizon is the fuel. For RES generation, none production nor cycling costs are considered.

2.4.2. Farm power limits

Rectangular capability is considered for farms [29]. Eqs. (19)–(22) model these limits. Fig. 6 illustrates this capability. Notice that $\overline{\mathrm{P}}_b, \underline{\mathrm{Q}}_g, \overline{\mathrm{Q}}_g$ of the farm depends on Patt_t, the considered wind/sun pattern.

$$0 \leqslant p_{bt}^{wi} \leqslant \mathrm{Patt}_t^{wi}\, \overline{\mathrm{P}}_b \quad \forall\, t > 1, b \in \mathrm{B}^{wi} \tag{19}$$

$$0 \leqslant p_{bt}^{pv} \leqslant \mathrm{Patt}_t^{su}\, \overline{\mathrm{P}}_b \quad \forall\, t > 1, b \in \mathrm{B}^{pv} \tag{20}$$

$$\mathrm{Patt}_t^{wi}\, \underline{\mathrm{Q}}_g \leqslant q_{bt}^{wi} \leqslant \mathrm{Patt}_t^{wi}\, \overline{\mathrm{Q}}_g \quad \forall\, t > 1, b \in \mathrm{B}^{wi} \tag{21}$$

$$\mathrm{Patt}_t^{su}\, \underline{\mathrm{Q}}_g \leqslant q_{bt}^{pv} \leqslant \mathrm{Patt}_t^{su}\, \overline{\mathrm{Q}}_g \quad \forall\, t > 1, b \in \mathrm{B}^{pv} \tag{22}$$

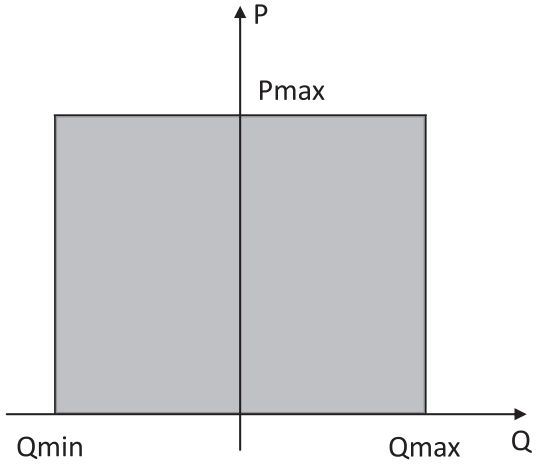

Fig. 6. RES rectangular capability.

2.4.3. Farm ramp limits

Usually, considering a ramp of 10% of the wind/solar power rate per minute, is industry practice [31]. For the time-step of 15 min of this work, ramp constraints are not binding, therefore, not considered.

2.5. Vertical interchange of energy

The interchange of energy between the TSO and the DSO is crucial for stability purposes and economic efficiency. From the technical point of view, the TSO is a strong link that can help stabilizing voltage or energy fluctuations as well as it can support the DSO with ancillary services. From the economic point of view, the TSO permits to make energy transactions to clear the electricity market efficiently. However, one of the main purposes of this work is to minimize this interaction to limit the effects of intermittency and randomness of RES in the higher level power system. Eq. (23) models the limits of energy interchange from/to the TSO.

$$\underline{VI}_b \leqslant p^{vi}_{bt} \leqslant \overline{VI}_b \quad \forall\, t>1, b \in B^{vi} \tag{23}$$

2.5.1. Penalization for vertical interchange deviation

To minimize the vertical interchange of energy, we implemented a penalty function which is added to the OF (fourth term). Eqs. (24)–(27) formulate the penalization function [29]. Fig. 7 schematizes it.

$$VI^{Pen} = \rho_{\omega_1} + \sum_{\omega>1}^{\omega_n} \alpha_\omega\, \Delta VI_\omega \quad \forall\, t>1, b \in B^{vi} \tag{24}$$

$$p^{vi} = \underline{VI} + \sum_{\omega>1}^{\omega_n} \Delta VI_\omega \quad \forall\, t>1, b \in B^{vi} \tag{25}$$

$$\Delta VI_\omega \geqslant 0 \quad \forall\, t>1, b \in B^{vi} \tag{26}$$

$$\Delta VI_\omega \leqslant p^{vi}_{\omega} - p^{vi}_{\omega-1} \quad \forall\, t>1, b \in B^{vi}, \omega>1 \tag{27}$$

2.6. Energetic balance

The energetic balance used considers both the active and reactive offer-demand-flow equations [29].

$$\begin{aligned} &p^{co}_{g\in b,t} + p^{bi}_{bt} + p^{wi}_{bt} + p^{pv}_{bt} + p^{ba}_{bt} + p^{ge}_{bt} + p^{hi}_{bt} + p^{vi}_{bt} + p^{vpp}_{bt} \\ &= d^{ac}_{bt} + dr_{bt} + p^{pu}_{bt} + d^{vpp}_{bt} + \sum_j pf_{b,j,t} \quad \forall\, b,t \end{aligned} \tag{28}$$

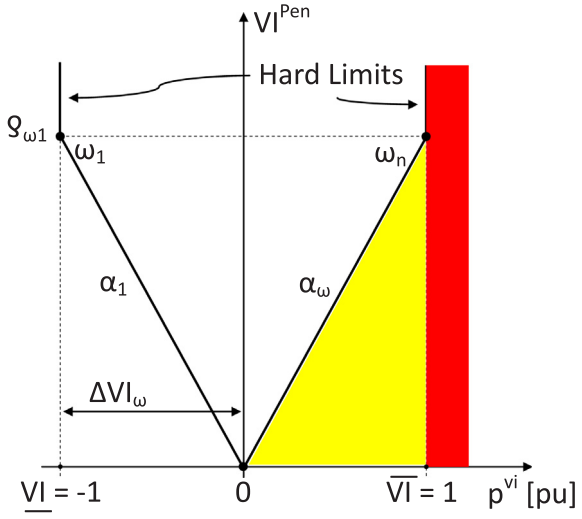

Fig. 7. Penalization for Vertical Interchange.

$$\begin{aligned} &q^{co}_{g\in b,t} + q^{bi}_{bt} + q^{wi}_{bt} + q^{pv}_{bt} + q^{ge}_{bt} + q^{vi}_{bt} \\ &= d^{re}_{bt} + \sum_j qf_{b,j,t} \quad \forall\, b,t \end{aligned} \tag{29}$$

Further explanation is needed regarding the definition of the terms $pf_{i,j,t}$ and $qf_{i,j,t}$. In the next section, these will be formally defined.

2.7. Reserve requirements

Reserve requirements are necessary for the reliable and robust operation of any power system and are essential in power grids with high penetration of RES. We considered that the reserve is contributed by the conventional generation units and the link between the DSO and the TSO. Eqs. (30)–(34) model the reserve requirements [29].

$$\sum_{g\in G^{res}} re_{gt} + \sum_{b\in B^{vres}} vre_{bt} \geqslant R \sum_{b\in B^{dem}} d^{ac}_{bt} \quad \forall\, t>1 \tag{30}$$

$$re_{gt} \leqslant u_{gt}\, \overline{P}_g - p^{co}_{gt} \quad \forall\, t>1 \tag{31}$$

$$p^{vi}_{bt} + vre_{bt} \leqslant \overline{VI} \quad \forall\, t>1 \tag{32}$$

$$0 \leqslant re_{gt} \leqslant \overline{P}_g - \underline{P}_g \quad \forall\, t>1, g \in G^{res} \tag{33}$$

$$0 \leqslant vre_{bt} \leqslant \overline{VI}_b \quad \forall\, t>1, b \in B^{vres} \tag{34}$$

3. Network model

To evaluate the integration of RES is essential to consider the physical limitations of the power grid. An accurate modeling for operation planning purposes would comprise an AC representation of the network [29]. However, a full AC representation for the specific application of this work would be computationally intractable. Therefore, it is needed an approximation that could balance between accuracy and computational tractability. We use a linear approximation of the AC network model which captures the main features and requirements of the scope of this work, under the assumptions that justify and validate its applicability:

- The model is appropriate for geographically dispersed small grids.
- Thermal limits are dominating constraints.
- Non-linearity can be linearized.
- Local voltage drop controls are available.
- Branch resistance values are negligible compared to reactance values.

The confidence on linearized power flow models depends strongly on the particular application and the representation of losses [32]. Some studies [33] justify the use of lossless models, estimating in 5% the error in line loadings, for techno-economic and planning purposes. This estimation is the assumption adopted in this work.

3.1. Linear network model

Eqs. (35) and (36) represent the Kirchhoff's nodal balances for the active and reactive parts of the power flows [29].

$$P_i = \sum_{j=1}^{J} |V_i||V_j|(G_{ij}\cos(\Delta\theta_{ij}) + B_{ij}\sin(\Delta\theta_{ij})) \tag{35}$$

$$Q_i = \sum_{j=1}^{J} |V_i||V_j|(G_{ij}\sin(\Delta\theta_{ij}) - B_{ij}\cos(\Delta\theta_{ij})) \tag{36}$$

It is assumed that the resistance of HV transmission circuits ($\geqslant$ 110 kV) is significantly less than the reactance. Thus, it is possible to approximate the conductance to zero and the susceptance to $-\frac{1}{x}$. Applying this to the power flow Eqs. (35) and (36):

$$P_i = \sum_{j=1}^{J} |V_i||V_j|(B_{ij}\sin(\theta_i - \theta_j)) \quad (37)$$

$$Q_i = \sum_{j=1}^{J} |V_i||V_j|(-B_{ij}\cos(\theta_i - \theta_j)) \quad (38)$$

It is assumed that for normal operating conditions the angular difference of voltage phasors between two buses, $\Delta\theta_{ij} = \theta_i - \theta_j$, is less than 10–15 degrees. Thus, the angular difference across any transmission circuit is small. Consider in Eqs. (37) and (38), that $\theta_i - \theta_j$ is the argument of trigonometric functions, as the angle $\theta_i - \theta_j$ gets smaller, the cosine function approaches 1 and the sine of a small angle is the angle itself when the angle is in radians. Applying these to Eqs. (37) and (38):

$$P_i = \sum_{j=1}^{J} |V_i||V_j|(B_{ij}(\theta_i - \theta_j)) \quad (39)$$

$$Q_i = \sum_{j=1}^{J} |V_i||V_j|(-B_{ij}) \quad (40)$$

Rearranging terms in Eq. (40):

$$Q_i = -|V_i|^2 b_i + \sum_{j=1, j\neq i}^{J} |V_i||b_{ij}|(|V_i| - |V_j|) \quad (41)$$

In the per-unit system, the numerical values of voltage magnitudes $|V_i|$ and $|V_j|$ are very close to 1. The typical range under normal operating conditions is 0.9 to 1.1. Then, it is assumed $|V_i| = |V_j| = 1.0$ everywhere they appear as a multiplying factor. Making this approximation results in:

$$P_i = \sum_{j=1, j\neq i}^{J} B_{ij}(\theta_i - \theta_j) \quad (42)$$

$$Q_i = -b_i + \sum_{j=1, j\neq i}^{J} |b_{ij}|(|V_i| - |V_j|) \quad (43)$$

Eqs. (42) and (43) represent the bus power balance for active and reactive components. Considering that the RHS of Eqs. (42) and (43) represents power flows, then the LHS represents the difference between the generated and demanded powers. Therefore, Eqs. (44) and (45) represent the active-reactive power flows from bus i to bus j, respectively.

$$pf_{i,j} = \gamma S'(\theta_i - \theta_j) \quad (44)$$

$$qf_{i,j} = -b_i^{shunt} + |b_{i,j}^{branch}|(|V_i| - |V_j|) \quad (45)$$

With the definition of Eqs. (44) and (45) is possible to construct the set of constraints regarding the branch network limits. Considering the coupled power flows $pf_{i,j}$ and $qf_{i,j}$ through any transmission system, Eq. (46) represents this coupling.

$$(pf_{i,j})^2 + (qf_{i,j})^2 = (|\overline{S_{i,j}}|)^2 \quad (46)$$

In the *P-Q* plane of Fig. 8, Eq. (46) represents a circle with radius $|\overline{S_{i,j}}|$. An approximation of a circle using polygonal inner approximation has been presented in [34], thus, the circle can be approximated by a n-sided convex regular polygon represented by Eq. (47).

$$\left[\sin\left(\frac{2\pi l}{n}\right) - \sin\left(\frac{2\pi}{n}(l-1)\right)\right] pf_{i,j} - \left[\cos\left(\frac{2\pi l}{n}\right) - \cos\left(\frac{2\pi}{n}(l-1)\right)\right] qf_{i,j} - |\overline{S_{i,j}}| \sin\left(\frac{2\pi}{n}\right) \leq 0 \quad (47)$$

Thus, the non-linear Eq. (46) is modeled with 4 linear Eqs. (47) as follows:

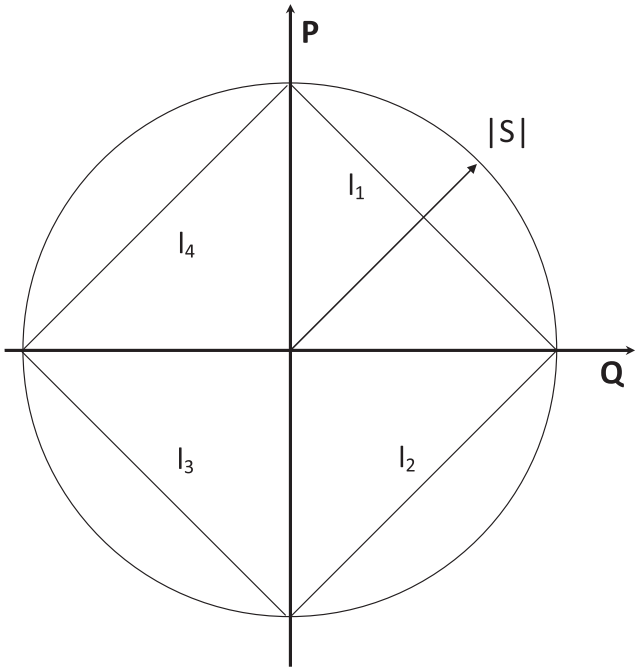

Fig. 8. *P-Q* plane.

$$pf_{i,j} + qf_{i,j} \leq |\overline{S_{pu}}| \quad (48)$$

$$pf_{i,j} - qf_{i,j} \leq |\overline{S_{pu}}| \quad (49)$$

$$-pf_{i,j} + qf_{i,j} \leq |\overline{S_{pu}}| \quad (50)$$

$$-pf_{i,j} - qf_{i,j} \leq |\overline{S_{pu}}| \quad (51)$$

Finally, the slack bus angle is set as the reference in Eq. (52) and the angle bounds are given in Eq. (53).

$$\theta_{bt} = 0 \quad b = slack \quad \forall\, t > 1 \quad (52)$$

$$-\pi \leq \theta_{bt} \leq \pi \quad b \neq slack \quad \forall\, t > 1 \quad (53)$$

3.2. Penalization for voltage deviation

To keep the voltage magnitude the nearest possible to the desired set point, for Example 1 [pu] value in Fig. 9, we implemented a linear piecewise penalization function [29]. Eqs. (54)–(57) formulates the function. This penalization function is only a mathematical tool and the

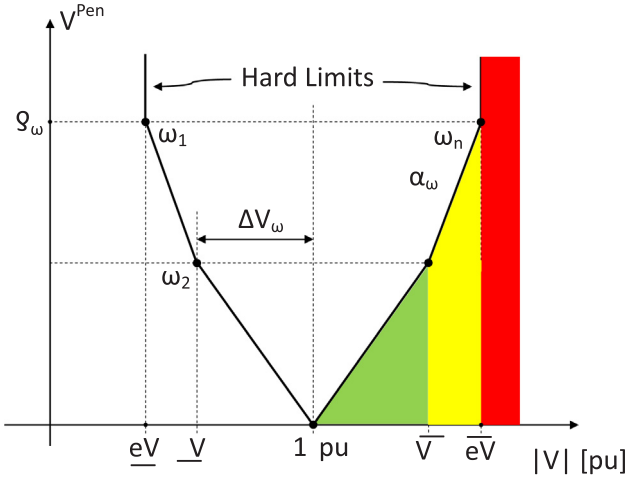

Fig. 9. Penalization of Voltage Magnitude Deviation.

penalization term V^{Pen} is added to the objective function, Eq. (1), to drive the solver to minimize deviations of the voltage magnitude from the set point. Setting different values for each bus is possible.

$$V^{Pen} = \rho_{\omega_1} + \sum_{\omega=1}^{\omega_n} \alpha_\omega * \Delta V_\omega \quad \forall\, b,t > 1 \tag{54}$$

$$|V| = \underline{eV} + \sum_{\omega>1}^{\omega_n} \Delta V_\omega \quad \forall\, b,t > 1 \tag{55}$$

$$\Delta V_\omega \geqslant 0 \quad \forall\, b,\omega,t > 1 \tag{56}$$

$$\Delta V_\omega \leqslant |V_\omega| - |V_{\omega-1}| \quad \forall\, b,\omega > 1,t > 1 \tag{57}$$

4. Flexibility options

Compared to conventional electricity sources, wind/solar based renewables have two particular drawbacks, they are intermittent and stochastic. These disadvantages imply that wind/solar power outputs cannot be modulated by the producers throughout the day, as they depend on meteorological conditions. As a result, the level of power production is not known beforehand with certainty, but can only be short-term forecasted with a certain accuracy. In turn, this implies that corrective measures may have to be taken with short notice to ensure the safety of power system operation.

Many flexibility options have been discussed in the literature to soften the variability of the renewable energy production. We evaluate the application of options already existent in the current grids or with potential to be incorporated. In this regard, this section describes the models of the different flexibility options used in this work.

4.1. Pumped Energy Storage System

Traditionally, Pumped Energy Storage System (PESS) are operated to allow shifting the demand in time. The operation consisted in producing electricity during high-demand/price periods and consuming it at low-demand/price periods. Naturally, this flexibility feature is not free, involving generally an efficiency ranging between 70% and 80%.

A mathematical model for the functioning of PESS is described by Eqs. (58)–(67) [29]. It is important to note that considering time periods different from one hour, obligates to make a distinction between power and energy.

$$p_{bt}^{ge} \leqslant u_{bt}^{ge}\, \overline{\mathrm{PG}} \quad \forall\, t > 1 \tag{58}$$

$$p_{bt}^{pu} \leqslant u_{bt}^{pu}\, \overline{\mathrm{PP}} \quad \forall\, t > 1 \tag{59}$$

$$u_{bt}^{ge} + u_{bt}^{pu} \leqslant 1 \quad \forall\, t > 1 \tag{60}$$

$$P_{bt}^{soc} = P_{b,t-1}^{soc} - \Delta t\, \eta\, p_{bt}^{ge} + \Delta t\, \eta\, p_{bt}^{pu} \quad \forall\, t > 1 \tag{61}$$

$$P_{bt}^{soc} = \mathrm{P}_0^{soc} \quad \forall\, t = T \tag{62}$$

$$p_{bt}^{pu} - p_{b,t-1}^{pu} \leqslant \mathrm{RU} \quad \forall\, t > 1 \tag{63}$$

$$p_{bt}^{ge} - p_{b,t-1}^{ge} \geqslant -\mathrm{RD} \quad \forall\, t > 1 \tag{64}$$

$$\underline{\mathrm{PE}} \leqslant P_{bt}^{soc} \leqslant \overline{\mathrm{PE}} \quad \forall\, t > 1 \tag{65}$$

$$p_{bt}^{ge}, p_{bt}^{pu} \geqslant 0 \quad \forall\, t > 1 \tag{66}$$

$$u_{bt}^{ge}, u_{bt}^{pu} \in \{0,1\} \quad \forall\, t > 1 \tag{67}$$

4.2. Battery Energy Storage System

Battery Energy Storage System (BESS) can perform spatiotemporal arbitrage of energy but at a much smaller power capability scale compared to PESS. BESS can be distributed conveniently or even moved among locations of the grid to alleviate network congestion and/or reduce wind/solar energy spillage. Another advantage of BESS is their high-efficiency values ranging from 80 to 90%.

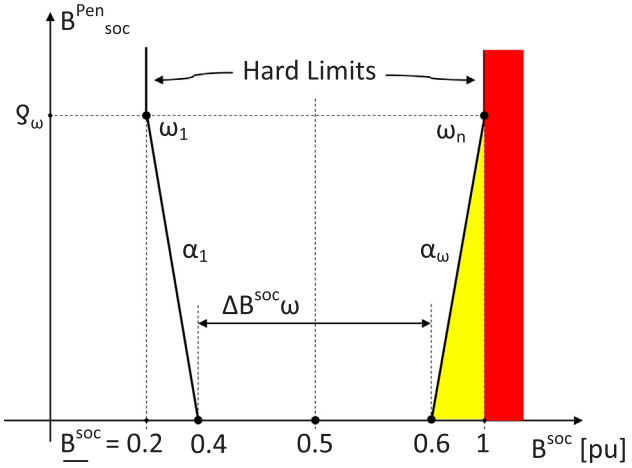

Fig. 10. Penalization of Battery State of Charge Deviation.

Compared to the PESS, the BESS model does not include binary variables to reduce the problem size. Instead, we permit the power variable ranging between negative and positive values. These limits are bounded by the maximum charging/discharging modes. It is assumed that the battery working temperature is kept constant. Following, the corresponding formulation [35].

$$B_{bt}^{soc} = B_{b,t-1}^{soc} + \Delta t\, \eta\, p_{bt}^{ba} \quad \forall\, b \in B^{ba},t > 1 \tag{68}$$

$$\underline{\mathrm{BE}} \leqslant B_{bt}^{soc} \leqslant \overline{\mathrm{BE}} \quad \forall\, b \in B^{ba},t > 1 \tag{69}$$

$$-\overline{\mathrm{BP}} \leqslant p_{bt}^{ba} \leqslant \overline{\mathrm{BP}} \quad \forall\, b \in B^{ba},t > 1 \tag{70}$$

4.2.1. Penalization for B^{soc} set point deviation

To keep the cycling stress of the battery to the minimum possible, we implemented a linear piecewise penalization function. Fig. 10 illustrates a generic penalization function. Eqs. (71)–(74) formulate the function [29]. The penalization term B_{soc}^{Pen} is added to the OF, Eq. (1), to drive the solver to minimize the cycling stress from the set point, in this case, 0.5 [pu].

$$B_{soc}^{Pen} = \rho_{\omega_1} + \sum_{\omega=1}^{\omega_n} \alpha_\omega\, \Delta B_\omega^{soc}\, \overline{\mathrm{BE}} \quad \forall\, b,t > 1 \tag{71}$$

$$B^{soc} = \underline{\mathrm{BE}} + \sum_{\omega>1}^{\omega_n} \Delta B_\omega^{soc}\, \overline{\mathrm{BE}} \quad \forall\, b,t > 1 \tag{72}$$

$$\Delta B_\omega^{soc} \geqslant 0 \quad \forall\, b,\omega,t > 1 \tag{73}$$

$$\Delta B_\omega^{soc} \leqslant B_\omega^{soc} - B_{\omega-1}^{soc} \quad \forall\, b,\omega > 1,t > 1 \tag{74}$$

4.3. Demand response

Demands can contribute to flexibility by many actions:

1. By shifting energy from peak demand to low demand periods.
2. By decreasing the peak demand.
3. By increasing the valley demand.
4. By reducing the rate of increase at periods of high demand increase.
5. By reducing the rate of decrease at periods of high demand decrease.

To unlock this potential flexibility, different initiatives have been proposed [36]; for example, dynamic pricing, time-of-use/interruptible tariffs, frequency/voltage-based controls and other market-based initiatives. However, influencing demands by a price signal is not new.

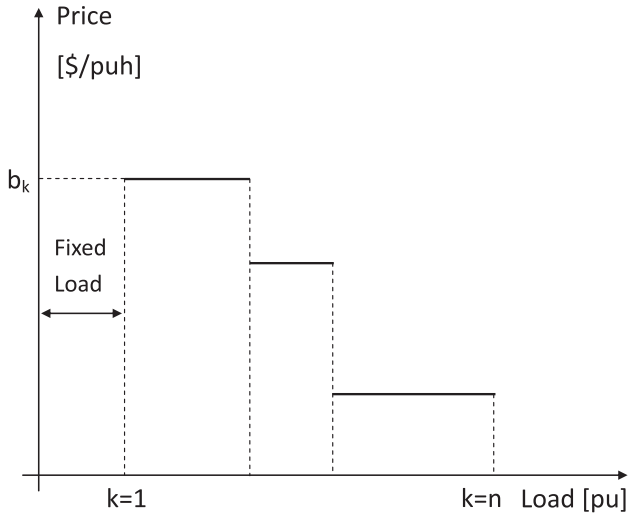

Fig. 11. Demand response function.

For example, time-of-use tariffs had played an important role influencing consumer behavior and shifting consumption in several countries. Nowadays, this price mechanisms are challenged as the penetration of RES into power systems grows sufficiently large to influence the electricity markets. Time-of-use tariffs are static, in a sense that they are fixed long time in advance, and therefore unable to adapt to the rapid fluctuations of RES. Stochastic production can lower market prices even during the peak hours of the day; then, the price signal must adapt dynamically to the forecast level of renewable output. Real-time dynamic pricing is meant to serve this purpose. Consequently, a deferrable load with multiple blocks (depending on price signals) is the model chosen in this work.

A demand function (deferrable with multiple blocks) that depends on price signals, λ_t, can be represented as a piecewise linear function. Fig. 11 illustrates the price energy block function. For example, anytime an increment of RES injection decreases the grid electricity price, λ_t, below the benefit value of the DR, be_k, the DR option can increment the consumption accordingly. Eqs. (75)–(78) formulate the demand response model [36]. Any consumption can be splitted into a fixed and a flexible component, $\{d_{bt}^{ac} + dr_{tk}\} \in b$.

$$dr_{tk} - dr_{t-1,k} \leqslant \mathrm{RU} \quad \forall\, tk \tag{75}$$

$$dr_{t-1,k} - dr_{tk} \leqslant \mathrm{RD} \quad \forall\, tk \tag{76}$$

$$\sum_{k=1}^{K} dr_{tk} \leqslant \overline{\mathrm{DR}}^{h} \quad \forall\, t \tag{77}$$

$$dr_{tk} \geqslant 0 \quad \forall\, tk \tag{78}$$

$\overline{\mathrm{DR}}^{h}$ is the upper bound to the demand response during a single period. Note, that the model can also consider load shedding when the *Fixed load* in Fig. 11 is set to null.

4.4. Virtual power plant

Currently, distribution grids are incorporating a large number of distributed resources. Consequently, the communication between them and the transmission system operator would be impracticable due to the high costs of the required information and technology capability. Instead, a decentralized management of aggregated distributed resources can potentially overcome the increase in complexity of the system operation. This decentralized management is the cornerstone of the concept of a Virtual Power Plant (VPP).

Technically, a VPP can be defined as a group of distributed generating units, flexible loads, and storage systems operating as an independent entity [37]. The primary purpose of a VPP is to coordinate the operation of the constituent parts, maximizing the profit. Also, a VPP can interact with the transmission system, offering support services regarding generation or demand.

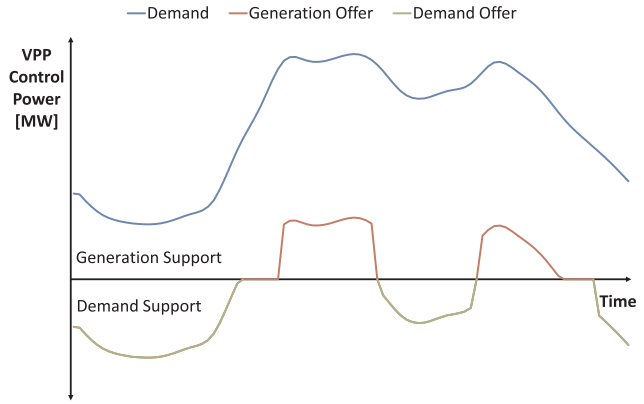

Fig. 12. Virtual Power Plant patterns.

In our model, we incorporate the VPP support services as patterns and price signals. These patterns can be observed in Fig. 12. We only consider generation and demand support services.

The variables p_{bt}^{vpp} and d_{bt}^{vpp} represent the generation and demand support services of the VPP. These variables are incorporated in the balance constraint, Eq. (28), and in the OF, Eq. (1). The terms added into the OF depend on the price signal λ_t of the grid. For example, when λ_t is negative, the market communicates a surplus of generation in the system and the VPP can offer additional demand depending on the relation between the λ_t signal and the availability of excess demand. On the other hand, when λ_t is positive, the market communicates a lack of generation in the system and the VPP can offer additional generation depending in the relation between the λ_t signal and the availability of excess generation.

The constraints (79)–(81) establish the limits for the VPP support services and the exclusion between generation or demand support.

$$0 \leqslant p_{bt}^{vpp} \leqslant ug_{bt}^{vpp}\,(\overline{\mathrm{VPP}}\ \mathrm{Patt}_t^{vpp}) \tag{79}$$

$$0 \leqslant d_{bt}^{vpp} \leqslant ud_{bt}^{vpp}\,(\underline{\mathrm{VPP}}\ \mathrm{Patt}_t^{vpp}) \tag{80}$$

$$ug_{bt}^{vpp} + ud_{bt}^{vpp} \leqslant 1 \tag{81}$$

$$ug_{bt}^{vpp}, ud_{bt}^{vpp} \in \{0,1\}$$

4.5. Horizontal energy interchanges

A system with full access to technical and economical data could centrally operate. Due to several reasons, different system operators coordinate actions in multi-regional electricity markets. In fact, the system operator of each interconnected area clears its market independently of other areas. Nevertheless, the different systems/areas usually make energy transactions with the adjacent areas, mainly for security reasons. With the advance of the smart grid concept, it is expected that the different operators could exploit the interconnections with neighboring areas to add flexibility to the grids. Under this scenario, we analyze in this section the potential of energy interchanges in the horizontal level; i.e., interchange of energy between DSOs as seen in Fig. 13.

4.5.1. Horizontal energy interchange evaluation

The capacity of interchanging energy between interconnected DSOs may be measured through a sensitivity analysis. Therefore, we evaluate the horizontal flexibility of the grid calculating the potential to export energy to neighbor grids.

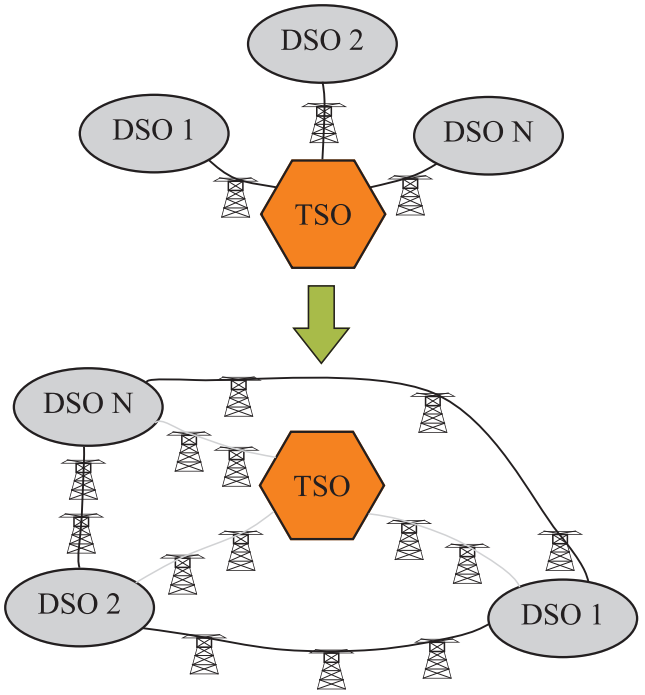

Fig. 13. Horizontal Energy Interchange.

The equality constraints, Eqs. (28), represent the balance of energy at each bus. These constraints impose that the Left Hand Side (LHS, usually generation) must equal the Right Hand Side (RHS, usually load). Without lack of generality, a simplified balance equation is like Eq. (82).

$$Generation + Flows = Load + Interchange \quad \forall\ tb \tag{82}$$

This set of equations, Eq. (82), can be perturbed to investigate changes in the optimal solution. If the *Interchange* is the only variable on the RHS and the LHS must compensate for the changes, then it is possible to measure how much the RHS can change before the solution loses its optimality. Consequently, for each time step it is possible to measure how much energy can be exported/imported in the form of a range on the RHS. Thus, for exporting energy:

$$Interchange \leqslant \overline{\text{RHS}} - Load \quad \forall\ t \tag{83}$$

An algorithm was developed to extract the maximum export/import hourly limits because shorter time steps can be challenging for horizontal energy transactions among DSOs. Fig. 14 represents an outline of the results obtained after a sensitivity calculation. For each time step, there are different power values; representing in the figure, the upper bound ranges for energy exports. The algorithm filters the four intra-hour values to a single one. In Fig. 14, the hourly limit for energy-export is represented by the red[1] line; i.e., the hourly limit is given by the nearest-to-zero intra-hour power value.

As it was mentioned in the first paragraph of this section, the calculation of quotas for exporting/importing energy through sensitivity analysis is valid for only one period. However, to evaluate the potential of horizontal energy interchanges between DSOs, it is necessary to obtain hourly transaction quotas for the entire scheduling horizon with a multi-variation of the RHS coefficients (*Interchanges*) that must not affect the optimal solution. Fortunately, there is a rule that allows simultaneous changes of RHS coefficients, called the "100% rule" [40]. Essentially, the rule states that the optimal solution remains unchanged for any simultaneous change that is a weighted combination of values

[1] For interpretation of color in Fig. 14, the reader is referred to the web version of this article.

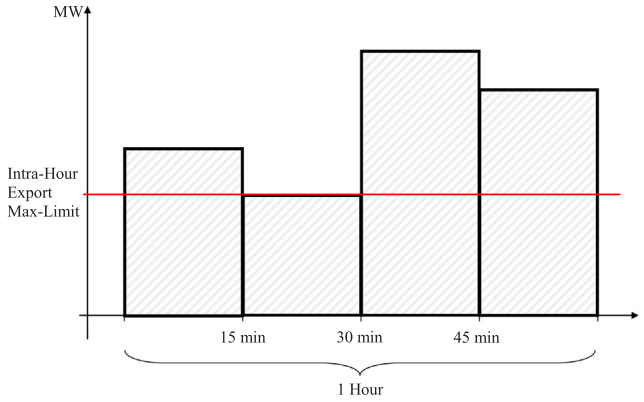

Fig. 14. Intra-hour Energy-export Values.

within the ranges of the RHS coefficients.

$$\sum_{t=1}^{T} \frac{\Delta \text{RHS}_t}{\Delta \overline{\text{RHS}}_t} \leqslant 1 \tag{84}$$

The fractions in the "100% rule" are the ratios of the actual change in a particular direction to the maximum possible change in that direction. In the particular case of export quotas, Eq. (84) transforms in:

$$\sum_{t=1}^{T} \frac{Interchange_t}{\overline{Export}_t} \leqslant 1 \tag{85}$$

Nevertheless, in this work, the goal is to evaluate how much energy can be exported to neighbor grids for the scheduling horizon. Thus, we formulate a maximization problem to calculate the corresponding export quotas as follows:

$$\max \sum_{t=1}^{T} Interchange_t \tag{86}$$

$$s.\ t.$$

$$\sum_{t=1}^{T} \frac{Interchange_t}{\overline{Export}_t} \leqslant 1 \tag{87}$$

The concept described in this section can be extended to develop an energy brokerage system [38] among different neighboring grids.

5. Experimental settings

This section illustrates the proposed methodology using a real power grid. For the ease of data presentation, all the tables in this section have power magnitudes. However, the model has been developed on the premise of the per unit system.

The model represented by Eqs. (1)–(81) is implemented in GAMS. The stopping criterion are gap = 5% or time = 600 s. The scheduling horizon is one month per each Winter, Summer and Autumn seasons. For balancing purposes, there is a requirement of 10% of reserve. The $\Delta t = 0.25$. The Δt is a conversion factor for costs data and power-energy relations. It is important to clarify what this parameter represents. Fig. 15 shows the conversion of 1 MWh to 0.25 MW$\frac{1}{4}$ h. Thus, every cost term and power-energy relation in the model have been converted with this Δt.

The following Tables 1–3 present the data corresponding to the penalty parameters for voltage deviations, battery state of charge deviations and vertical interchange deviations.

5.1. Power grid data

The power grid is extracted from a region of the 110 kV interconnected network on Germany [39]. The system data is shown in Tables 4–8. Fig. 16 describes the system one-line diagram. Table 5

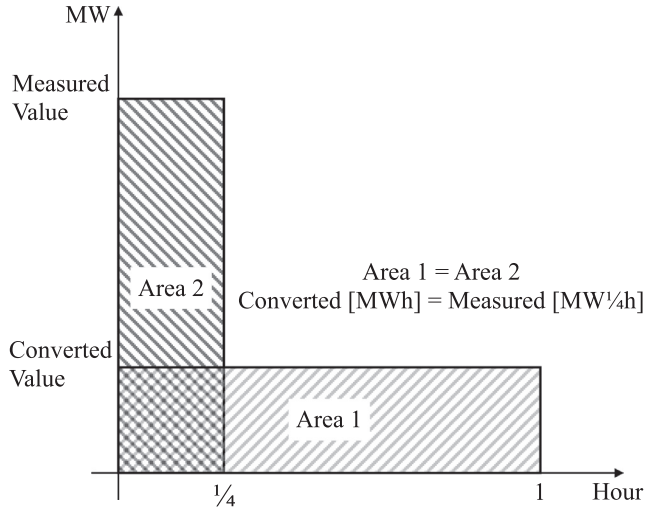

Fig. 15. Δt conversion factor illustration.

Table 1
Voltage deviations data.

ρ_ω			α_ω		ΔV_ω		
ω_1 [$/pu$\frac{1}{4}$h]	ω_2	ω_3	ω_{1-2} [nu]	ω_{2-3}	ω_1 [MW]	ω_2	ω_3
1	0	1	−10	10	0.9	1	1.1

Table 2
Battery state of charge deviations data.

	ρ_ω				α_ω		ΔB_ω^{soc}			
Bus	ω_1 [$/pu$\frac{1}{4}$h]	ω_2	ω_4	ω_5	ω_{1-2} [nu]	ω_{4-5}	ω_1 [%]	ω_2	ω_4	ω_5
b07	1	0	0	1	−50	25	20	40	60	100
b08	1	0	0	1	−66	33	20	40	60	100

Table 3
Vertical interchange deviations data: 250[$/MWh].

ρ_ω			α_ω		p_ω^{vi}		
ω_1 [$/pu$\frac{1}{4}$h]	ω_2	ω_3	ω_{1-2} [nu]	ω_{2-3}	ω_1 [MW]	ω_2	ω_3
6250	0	6250	−6250	6250	−100	0	100

Table 4
Line Data.

	Line	1	2	3	4	5	6	7
X	[pu]	.066	.050	.022	.056	.073	.009	.004
Rate	[MW]	104	138	46	25	25	25	25
	Line	8	9	10	11	12	13	14
X	[pu]	.047	.047	.037	.056	.030	.027	.044
Rate	[MW]	25	25	76	76	52	52	52

contains the peak load values at each bus; these values are respectively normalized with the load patterns. Notice that in Table 6 the Bio generators are considered as conventional in the sense they are controllable. The power grid is interconnected with the TSO at bus 1.

Table 5
Load Data.

	Industrial Load		Household Load		Voltage Limits	
Bus	MW	MVAR	MW	MVAR	Max [pu]	Min [pu]
2	1	0.75	1	0.48	1.1	0.9
3	0.5	0.37	1	0.48	1.1	0.9
5	3.1	2.33	3.1	1.5	1.1	0.9
6	2	1.5	6	2.9	1.1	0.9
10	3	2.25	7	3.4	1.1	0.9
11	4	3	10	4.8	1.1	0.9
12	3	2.25	6	2.9	1.1	0.9
13	4	3	5	2.4	1.1	0.9

Table 6
Conventional Generation Data.

		MW Limits		MVAR	Cost Coef.	Startup Costs
Bus	Label	Max	Min	Limits	[$/pu$\frac{1}{4}$h]	hot/warm/cold [$]
5	Bio	0.5	0.45	±0.4	3500	–
6	Conv	150	15	±100	2250	2850/3600/4800
11	Bio	0.3	0.27	±0.2	4500	–
13	Bio	5	4	±4	1250	–

Table 7
Renewable Generation Data.

Bus	Label	MW Max	MVAR Limits
2	PV	0.4	±0.32
3	PV	0.2	±0.16
5	PV	0.1	±0.08
7	WI	38	–
8	WI	28	–
10	PV	0.2	±0.16
11	PV	0.4	±0.32
12	WI	0.2	–
	PV	0.3	±0.24
13	WI	87	–
	PV	3	±2.4

Table 8
Pump Station Data.

Energy		Rate	Efficiency		Ramps	Ini.
Max [MWh]	Min	Pum./Gen. [MW]	Pum. [%]	Gen.	Up/Down [MW/min]	SOC [MWh]
600	40	80	85	72	7	300

5.2. Wind, solar, and load patterns data

We represent the system demand and the wind/solar power availability using a set of plausible scenarios based on historical data (2005–2016) of the power system of Germany [41]. Wind/solar/demand data (15-min length) are obtained from [41]. Normalized production values characterize the wind/sun availability where farms are located. On the other hand, we use characteristic demand profiles of the grid. Thus, we have patterns that correlate demand and RES production at each bus of the grid. A simulation scenario is an operating horizon which has information about demand and RES production for the corresponding season of the year. To attain computational tractability, we filter the possible scenarios for representative monthly patterns. This selection allows maintaining the spatial and temporal correlations among wind/solar and demand data. Thus, we select one representative

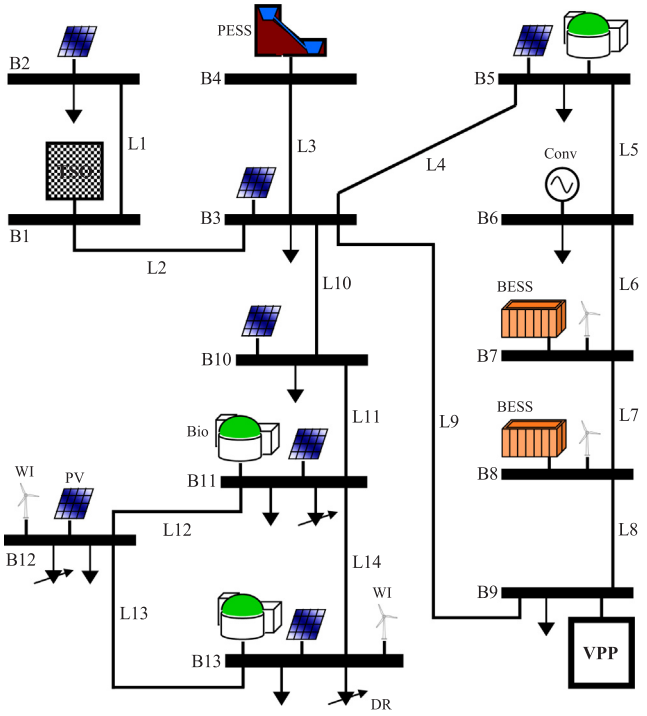

Fig. 16. Power Grid Diagram.

month January, July, and October for each season winter/summer/autumn respectively.

In this work, we are interested in a planning method to analyze the flexibility of the grid to better exploit the surplus of RES generation. We are mainly focused on maximal scenarios because this kind of RES scenarios submits the grid to a maximal stress. In this way, we would be able to extract important conclusions, very relevant to the system operators and market agents. Based on trustworthy statistical data published in [41], and having analyzed the corresponding RES patterns, we concluded that the autumn season contributed more significantly to the RES generation compared with the spring season along the 11 years period. This seasons behavior and for the sake of the article briefness, helped us to decide not to include the spring season results. We think it would produce information overload and also will extend the article unnecessarily. The utilization of typical scenarios do not produce a lack of generality of the methodology. On the contrary, the methodology results can help to infer general behavior patterns of power grid flexibility.

5.3. Pump station data

Currently in Germany exists several proposals to install pumping station power based on cavern reservoirs. Thus, we consider the possibility of installing 1 PESS at bus 4, whose characteristics are given in Table 9.

Table 9
Pump Station Data.

Energy		Rate	Efficiency		Ramps	Ini.
Max [MWh]	Min	Pum./Gen. [MW]	Pum. [%]	Gen.	Up/Down [MW/min]	SOC [MWh]
400	20	40	85	72	7	200

Table 10
Battery Energy Storage Systems Data.

Bus	Energy Max [MWh]	Min	Rate [MW]	Efficiency Cha./Dis. [%]	Ini. SOC [MWh]
7	40	8	20	90	20
8	40	8	20	90	20

Table 11
Grid load with demand response

	MW		Utility [$/pu$\frac{1}{4}$h]	
Bus	Max	Min	b_{k_1}	b_{k_2}
11	1	0.5	3000	2000
12	0.75	0.375	4000	3000
13	1	0.5	7000	4000

5.4. Battery data

We consider the possibility of installing 2 BESS, whose characteristics and locations are given in Table 10.

5.5. Demand response data

We consider 3 industries with the possibility to implement DR mechanisms, whose characteristics and locations are given in Table 11. The price λ_t for 2013 is extracted from [41].

5.6. Virtual power plant data

The generation support offer depends on the RES availability, on stored energy and conventional units. Consequently, we considered that the generation surplus exists when the price signals are positive. The demand support offer strongly depends on industrial loads; thus, we considered that a surplus demand exists whenever the price signals are negative. Data concerning maximum generation and demand support is presented in Table 12.

6. Numerical results

Results regarding power flows or voltage magnitudes are not presented in this section as they all remain inside the allowed limits. Results concerning RES energy are only analyzed for the wind farms because they have the largest share of the RES capacity in the grid.

6.1. Base case

This case has no flexibility options and represents the benchmark from which the rest of the simulation cases will be compared. Fig. 17 (Table A.16) present the main results for this case.

Results in Fig. 17 show that in winter only the 42.7% of the available RES energy is exploited, in summer the 72.4% and in autumn only the 31%. We discuss in the next paragraphs the particular conditions for each season.

In the winter month, there are three periods with high availability

Table 12
Virtual Power Plant Data.

Bus	Generation Support $\overline{VPP}$ [MW]	Demand Support $\underline{VPP}$ [MW]
9	25	50

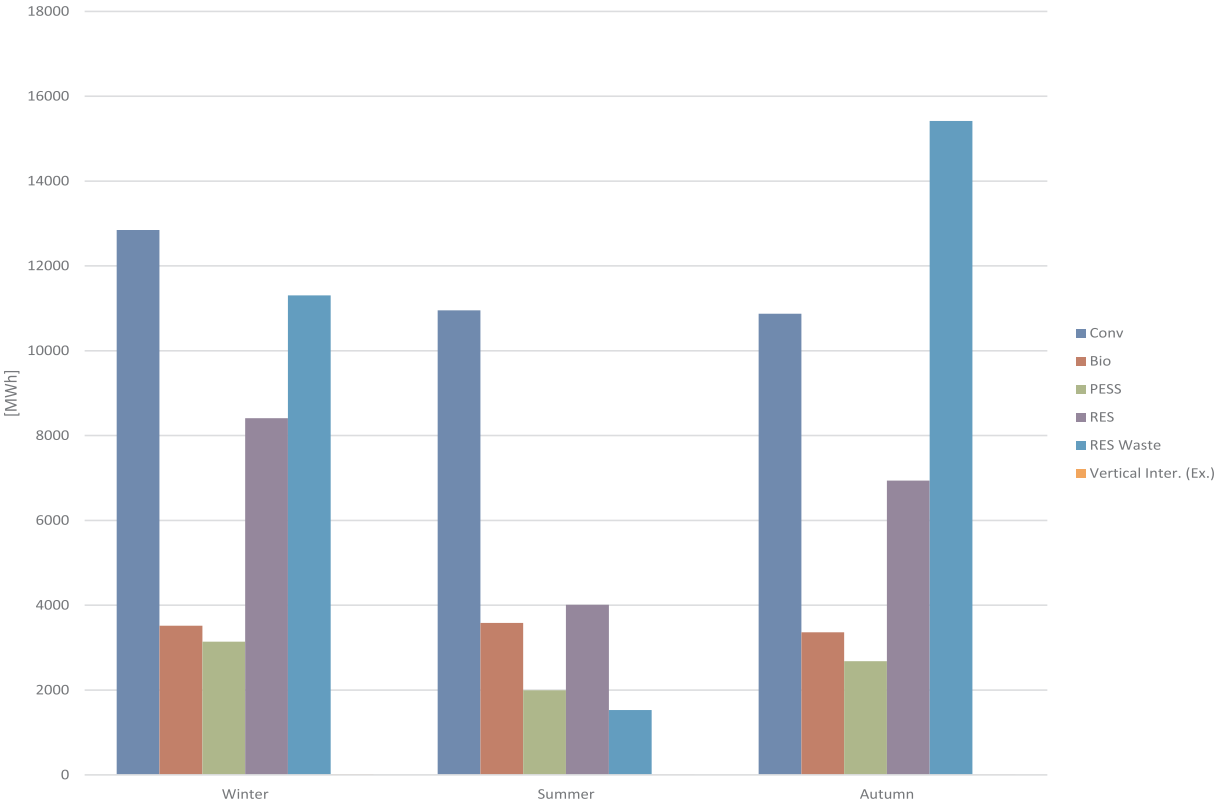

Fig. 17. Base Case.

of wind power. Period 1 between days 1–3. Period 2 between days 17–19. Period 3 between days 25–28. The curtailment of RES energy is also the highest in these three periods. For the rest of the month, almost 100% of the available RES energy is exploited. Between days 1–3 the available wind energy is 2705 MWh. Between days 17–19 is 4544 MWh and between days 25–28, 7108 MWh. These 3 Periods represent the 73% of the available winter wind energy.

The summer season is the worst regarding wind power availability, nevertheless, in the summer month, there are 4 periods with relatively high availability and curtailment of wind power. Period 1 for day 1; Period 2 between days 10–11; Period 3 between days 19–24; and Period 4 for day 28. For day 1 the available wind energy is 582 MWh. For Periods 2 and 3 the available wind energies are 575 MWh and 1515 MWh respectively. For day 28 is 453 MWh. These 4 Periods represent the 63% of the available summer wind energy.

In the autumn month there are six periods with high availability and curtailment of wind power. The fourth most important are: Period 1 between days 1–5; Period 2 between days 17–18; Period 3 between days 19–24; and Period 4 between days 25–28. Between days 1–5 the available wind energy is 4785 MWh. Between days 17–18 is 2105 MWh. Between days 19–24 is 4893 MWh and between days 25–28, 6499 MWh. These 4 Periods represent the 82% of the available autumn wind energy. Fig. 18 shows in detail Period 4 (Autumn) where the curtailment of RES energy is the highest.

The results show that the Periods with the highest wind availability represent the 73% in winter, 63% in summer and 82% in autumn. Also, these Periods coincide with the highest curtailment of RES energy. This fact leads to infer that what occur within these Periods establishes the general tendency for the rest of the seasons. Therefore, this can explain why only 42.7% of RES energy is exploited in winter, 72.4% in summer and 31% in autumn.

Summarizing, a series of complex interactions between high wind power availability and low demand, particularly in the mentioned periods, are some of the reasons that cause a large curtailment of RES

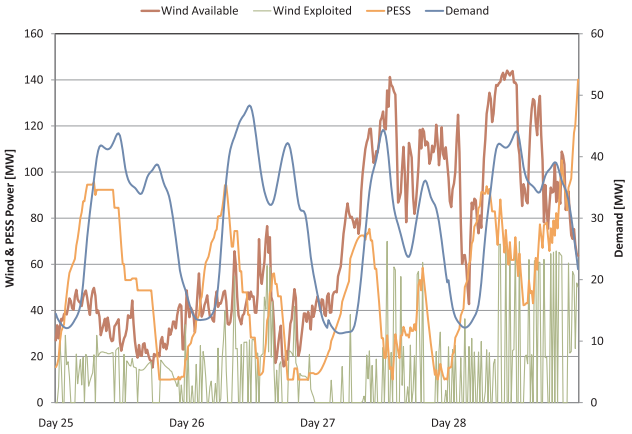

Fig. 18. Autumn: Days 25–28.

energy in all the seasons. It is also observed that the PESS is storing energy during these periods when the demand is low. However, the PESS is located far away from the main wind farms (buses 7, 8, 13) which reduces the possibility to store energy. Regarding the network, the line 3–4 is the only one reaching its thermal limits in 16 out of 720 h in the winter month, 2.5 h in summer and 18 in autumn.

6.2. Pump station case

This case incorporates the planned PESS expansion. Fig. 19 (Table A.17) present the results for this case.

Again, the Periods of maximum curtailment of RES are the same as the ones found in the base case. However, results in Fig. 19 show that now in winter the 45% of the available RES energy is exploited, representing an increase of 2.3% compared to the base case. In summer an 82% is exploited and in autumn a 34%, an increase of 9.6% and 3%

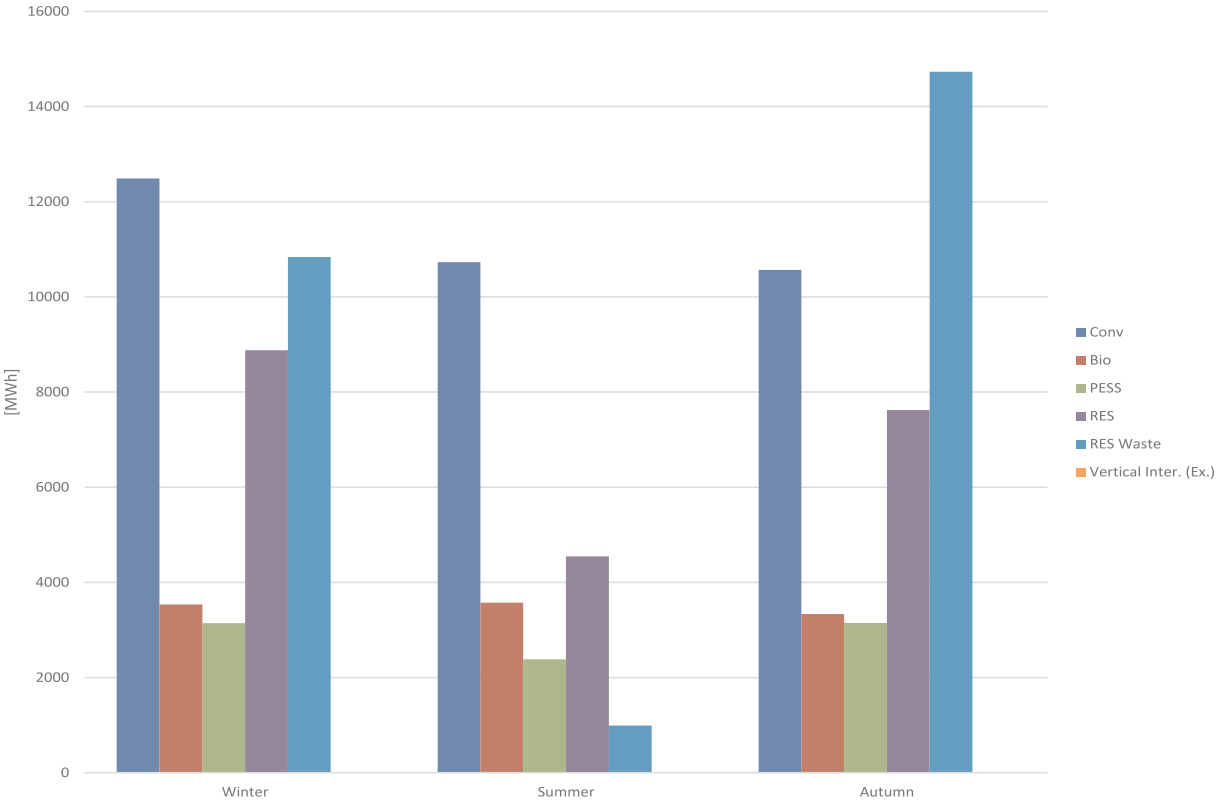

Fig. 19. PESS Case.

respectively.

Compared to the base case the curtailment of RES energy in winter is reduced 2% between days 1–3, an additional 2% between days 17–19, and 10% between days 25–28. Compared to the base case the curtailment of RES energy in summer is reduced 10.8% on day 1, 18.4% between days 10–11, 17.7% between days 19–24, and 23.2% on day 28. Compared to the base case the curtailment of RES energy in autumn is reduced 1.6% between days 1–5, 6.1% between days 17–18, 2% between days 19–24, and 2.5% between days 25–28. Fig. 20 shows in detail Period 4 (Autumn) where the curtailment of RES energy is still the highest.

Results show that the benefit of incorporating extra energy storage, in this case as new PESS power capacity (50% more), is evident. This benefit can be confirmed by an improvement of a 15% on the RES energy exploitation compared to the base case and it should be noted that this is achieved in only 3 months of a year. In this case, line 3–4

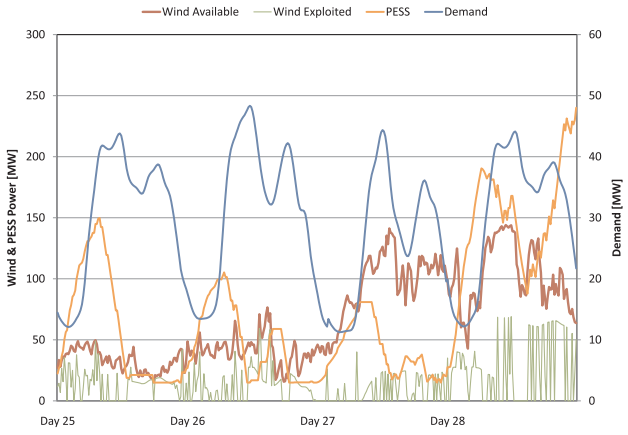

Fig. 20. PESS Autumn: Days 25–28.

(connecting PESS with the rest of the grid) has reached its thermal limits in 22.5 out of 720 h in the winter month, 3 h in summer and 24.5 in autumn. The PESS operation could give a better performance if this line is reinforced. In the next section, we will evaluate how BESS, distributed energy storage resources, behaves compared to the PESS concentrated storage.

6.3. Battery station case

This case incorporates the planned BESS. Fig. 21 (Table A.18) present the results for this case.

The Periods with the maximum waste of RES are the same as the base case. Results in Fig. 21 show that now in winter the 46.5% of the available RES energy is exploited, representing an increase of 3.8% compared to the base case. In summer an 87.3% is exploited and in autumn a 39.4%, an increase of 14.9% and 8.4% respectively.

Compared to the PESS case the waste of RES energy in winter is reduced 3.6% between days 1–3, an additional 2.6% between days 17–19, but the waste is increased 6.4% between days 25–28. Compared to the PESS case the waste of RES energy in summer is reduced 6.8% on day 1, 3.9% between days 10–11, 2.7% between days 19–24, and increased 2.9% on day 28. Compared to the PESS case the waste of RES energy in autumn is reduced 7.4% between days 1–5, 1.2% between days 17–18, 7.3% between days 19–24, and 4.8% between days 25–28. Fig. 22 shows in detail Period 4 (Autumn) where the waste of RES energy is still the highest.

Results show the benefits of incorporating distributed energy storage resources in comparison with centralized PESS. Compared to the PESS case, the new BESS helped to exploit 47.9% of the available RES energy on the three months analyzed, representing a 3.7% exploitation increment for the BESS case and a 7.3% increment compared to the base case. Notice that the energy-to-power ratio for each BESS is 2 and for the PESS expansion is 10 and that both options have the same power rate. Regarding the network state, again line 3–4 is the only one

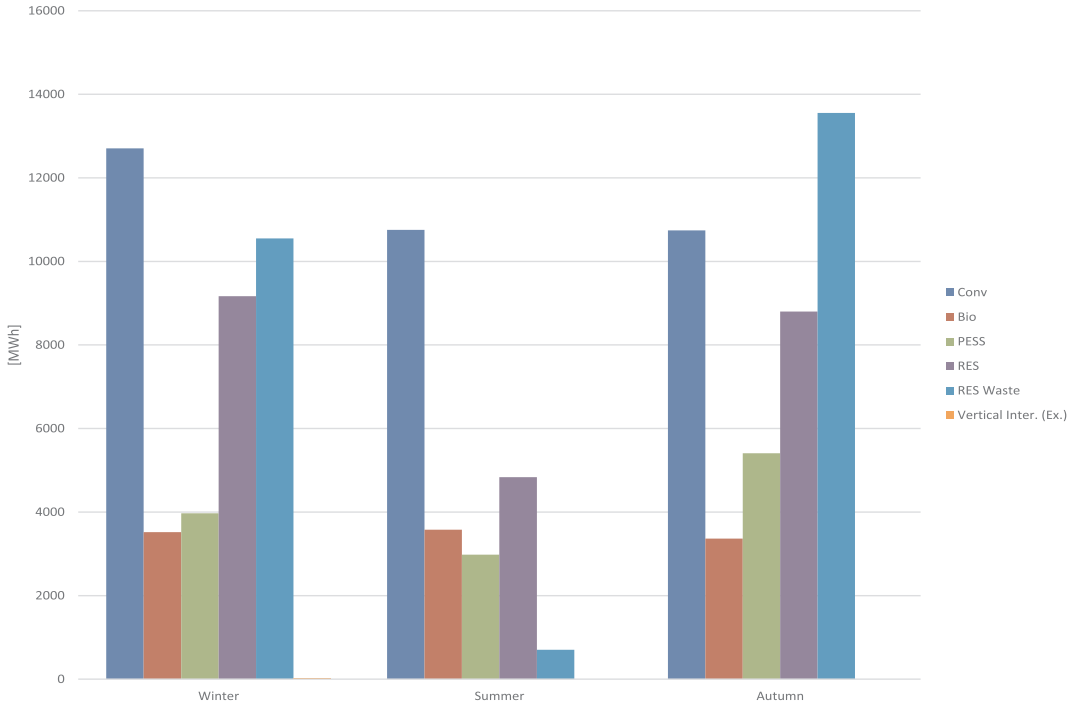

Fig. 21. BESS Case.

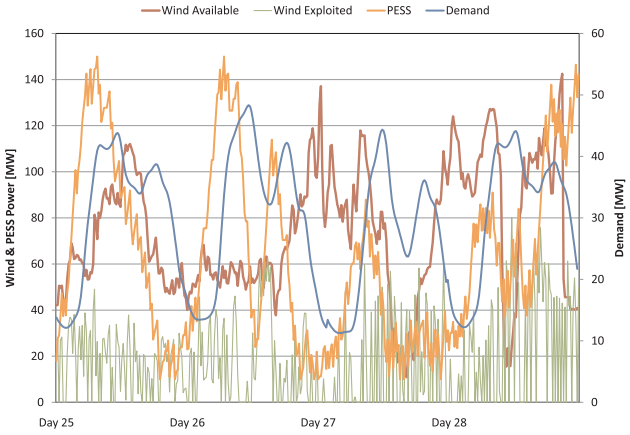

Fig. 22. BESS Autumn: Days 25–28.

reaching its thermal limits in 60 out of 720 h in the winter month, 13 h in summer and 94 in autumn. Compared to the PESS and base cases, it can be clearly seen in the BESS case that line 3–4 has significantly increased the number of hours when its thermal limit is reached. This increment can be explained by the increase in the RES injection to the grid and the batteries operation.

6.4. Demand response Case

This case incorporates the planned DR scheme. Fig. 23 (Table A.19) present the results for this case.

Results in Fig. 23 show that now in winter the 54.5% of the available RES energy is exploited, representing an increase of 11.8% compared to the base case. In summer a 94% is exploited and in autumn a 53.1%, an increase of 21.6% and 22.1% respectively.

Figs. 24 and 25 show in detail Period 4 (Autumn) where the waste of RES energy is the highest. The figure shows the interactions among the different DR, the demand pattern and the λ price signal for the period between days 25–28.

The DR helped to exploit 58.5% of the available RES energy on the three months analyzed, representing a 17.9% exploitation increment compared to the base case. Regarding the network state, again line 3–4 is the only one reaching its thermal limits in 24 out of 720 h in the winter month, 1 h in summer and 24.5 in autumn. Until now, this case represents the best flexibility option to be incorporated in the grid, based on the highest percentage of RES energy exploited and a network stress comparable to the PESS case.

6.5. Virtual power plant case

This case incorporates the planned VPP. Fig. 26 (Table A.20) present the results for this case.

Results in Fig. 26 show that now in winter the 50% of the available RES energy is exploited, representing an increase of 7.3% compared to the base case. In summer a 86% is exploited and in autumn a 34.5%, an increase of 13.6% and 3.5% respectively.

Fig. 27 shows the VPP patterns for additional demand and generation contribution in the period between days 10–11 (Summer) where the waste of RES energy is the minimum.

The VPP helped to exploit 46.9% of the available RES energy on the three months analyzed, representing a 6.3% exploitation increment compared to the base case. Regarding the network state, line 3–4 reached its thermal limits in 22 out of 720 h in the winter month, 2.5 h in summer and 22 in autumn.

6.6. Full case

This case incorporates all flexibility options. Fig. 28 (Table A.21) present the results for this case.

Again, the Periods of maximum waste of RES are the same as the ones found in the base case. Results in Fig. 28 show that now in winter the 64.2% of the available RES energy is exploited, representing an increase of 21.5% compared to the base case. In summer an 99.3% is exploited and in autumn a 62.9%, an increase of 26.9% and 31.9% respectively.

Compared to the base case the waste of RES energy in winter is reduced 42.3% between days 1–3, an additional 22.8% between days 17–19, and 18.8% between days 25–28. Fig. 29 shows in detail Period 3

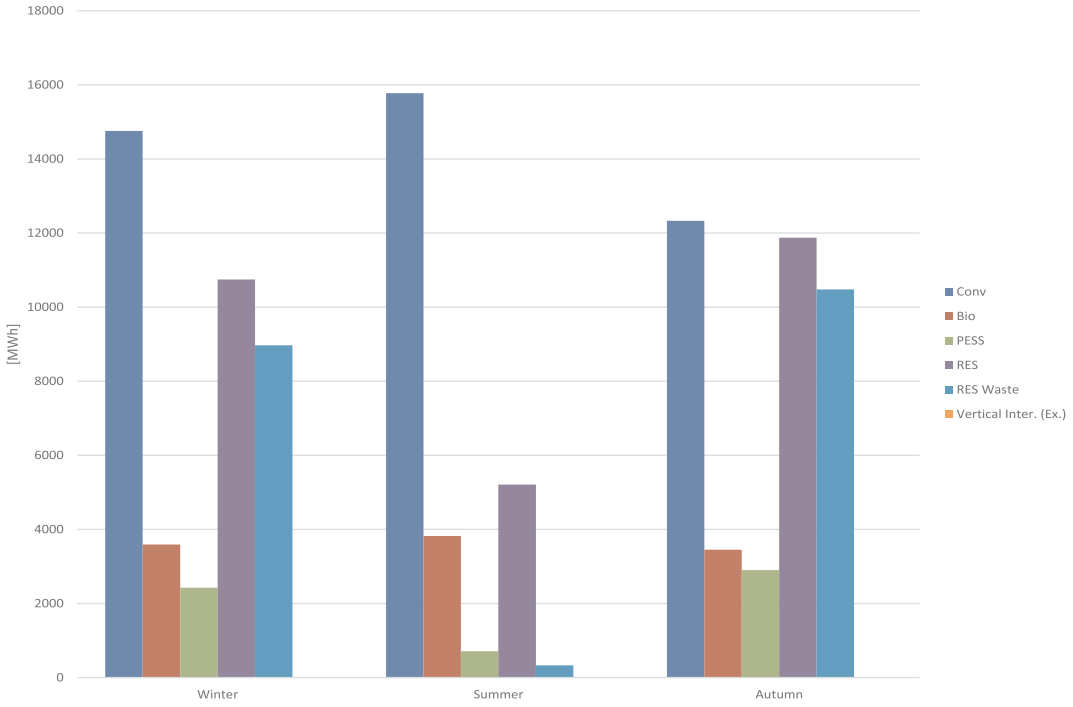

Fig. 23. DR Case.

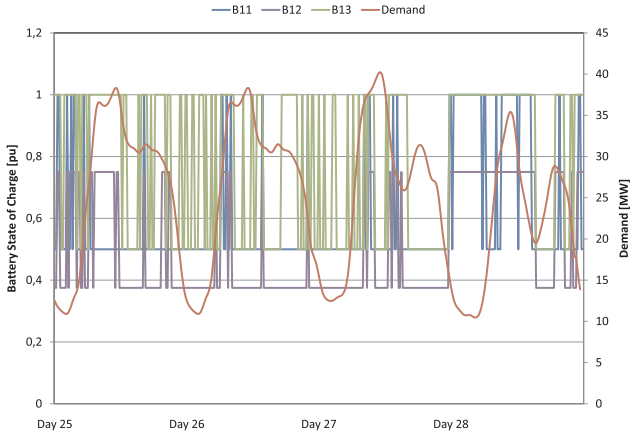

Fig. 24. DR Autumn: Days 25–28.

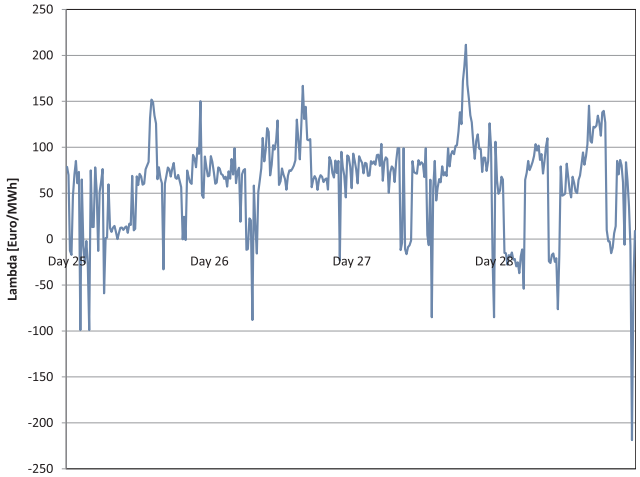

Fig. 25. Lambda Autumn: Days 25–28.

(Winter) where the waste of RES energy is now the highest.

Compared to the base case the waste of RES energy in summer is reduced 60% on day 1, 30% between days 10–11, 44% between days 19–24, and 62% on day 28. Compared to the base case the waste of RES energy in autumn is reduced 36.8% between days 1–5, 31.3% between days 17–18, 38.7% between days 19–24, and 25.2% between days 25–28.

Results show the benefit of combining all the flexibility options. The integration of RES is the largest compared to any other single option. This benefit can be confirmed by a total RES exploitation of an 67.7%. For this case, line 3–4 has reached its thermal limits in 68 out of 720 h in the winter month, 2 h in summer and 95 in autumn.

6.7. Resume of the results

Table 13 presents the resume of RES exploitation regarding all the cases. The results in the table show that all the flexibility options have the capacity to integrate, in a mayor extent, the RES energy into the power grid. However, it is reasonable to obtain different RES integration levels with the incorporation of the different flexibility options. To facilitate the analysis, we have divided the flexibility options in two groups. The first one conformed by the plausible options, i.e., these options need no mayor investments or modifications on the actual power grid; for example, DR and VPP. The second one conformed by the onerous options, i.e, they need further investments or modifications of the grid; for example, PESS and BESS.

From the results can be concluded that the best option to integrate RES is the incorporation of all the flexibility options. On the other hand, the worst option in terms of RES integration seems to be the PESS expansion. Also in terms of RES integration, BESS and VPP options seem to have a quite similar impact.

In our work, the plausible options (DR and VPP), coincidentally present the best RES integration figures compared to the onerous options. Thus, it is reasonable to conclude that these options have the mayor potential for the short-term application. These results, lead us to infer that although technological advances like storage resources are in vogue and certainly are going to be incorporated, it is also strongly recommendable to analyze existent options which, with minor

Table 13
Resume of the results.

Case	Season	RES Exploitation Season [%]	RES Exploitation Total [%]
Base	Winter	42.7	40.6
	Summer	72.4	
	Autumn	31	
PESS	Winter	45	44.2
	Summer	82	
	Autumn	34	
BESS	Winter	46.5	47.9
	Summer	87.3	
	Autumn	39.4	
DR	Winter	54.5	58.5
	Summer	94	
	Autumn	53.1	
VPP	Winter	50	46.9
	Summer	86	
	Autumn	34.5	
Full	Winter	64.2	67.7
	Summer	99.3	
	Autumn	62.9	

Table 14
Horizontal integration: DSO energy transactions.

Case	Season	RES potential for: Energy Export [MWh]	RES potential for: Curtailment Reduction [%]	New Total RES Exploitation [%]	RES Exploitation Increment [%]
Base	Winter	4389	38.8	64.7	22
	Summer	3607	100	100	–
	Autumn	4706	30.5	52	21
PESS	Winter	4965	45.8	70	25
	Summer	3123	100	100	–
	Autumn	4267	28.9	53	19
BESS	Winter	2963	28.0	61.5	15
	Summer	3072	100	100	–
	Autumn	3062	22.6	53.4	14
DR	Winter	4326	48.2	76.5	22
	Summer	5723	100	100	–
	Autumn	4768	45.5	74.1	21
VPP	Winter	4584	46.5	73	23
	Summer	4265	100	100	–
	Autumn	4457	30.4	54.5	20
Full	Winter	3742	53.0	83.2	19
	Summer	3312	100	100	–
	Autumn	2853	34.4	75.9	13

Table 15
DSO-TSO Control Power Allowance.

Case	Season	Energy Export [MWh]	Energy Import [MWh]	RES curtailment when: Export [%]	RES curtailment when: Import [%]
Full	Winter	6404	6569	10.7	34.7
	Summer	10	8634	0	0
	Autumn	8603	2670	8.7	36.5

Table A.16
Base Case.

Season	Total Generation Conv [MWh]	Bio	PESS	RES	RES Curtailment	Vertical Inter. Im.	Ex.
Winter	12,848	3518	3141	8409	11,307	–	8.8
Summer	10953	3583	1992	4010	1528	–	1.6
Autumn	10874	3363	2681	6937	15,418	–	4.3

Table A.17
PESS Case.

Season	Total Generation Conv [MWh]	Bio	PESS	RES	RES Curtailment	Vertical Inter. Im.	Ex.
Winter	12489	3537	3141	8879	10837	–	4.3
Summer	10731	3573	2381	4548	990	–	2
Autumn	10569	3336	3146	7623	14731	–	4.9

modifications, can even offer better flexibility capacity to the existent power grid.

In all cases, the autumn season seems to be the period of the year when the RES waste is the biggest. In this regard, the PESS can be programmed to its minimum storage level right before the beginning of the autumn season.

6.8. Horizontal integration: DSO-DSO sensitivity analysis

Applying the methodology presented in Section 4.5, in this section we analyze the potential to interchange energy in the horizontal level, i.e., to establish hourly energy transactions with a neighboring DSO at bus 9. Table 14 presents the results for all the cases.

Column 4 (RES potential for Waste Reduction) on Table 14 represents the percentage of energy that can be reduced from the column RES Waste on Tables A.16,A.17,A.18,A.19,A.20,A.21.

The new aggregated RES exploitation values are 62.9% for the Base case, 65.7% for the PESS, 62% for the BESS, 78.2% for the DR, 67.5% for the VPP, and 81.6% for the Full case. Compared to the previous cases these values represent increments of 22.3% for Base case, 21.5% for the PESS, 14.1% for the BESS, 19.7% for the DR, 20.6% for the VPP, and 13.9% for the Full. Therefore, DSO-DSO energy transactions have a great potential to diminish the RES waste. Particularly, in the plausible cases, DR and VPP flexibility options.

6.9. Vertical integration: DSO-TSO control power allowance

Similar to the independent VPP behavior, a DSO can evaluate how much generation-demand power control can offer to the TSO. This evaluation is particularly important because the TSO can require flexibility services from the DSOs. In this section, we analyze the range of DSO power controls offered to the TSO.

The methodology applied to calculate the control power allowance is based on the same model represented by Eqs. (1)–(81); nevertheless, for the allowance calculation we did not consider penalization (Eqs. (24)–(27)) for the vertical energy interchanges.

Table 15 presents the results for the control energy allowance from the DSO to the TSO, only for the Full case. Figs. 30 and 31 present the control energy allowance patterns for the three seasons.

Column Energy Export on Table 15, refers to the available energy to be delivered from the DSO to the TSO in the corresponding season. Column Energy Import refers to the energy that can be received by the

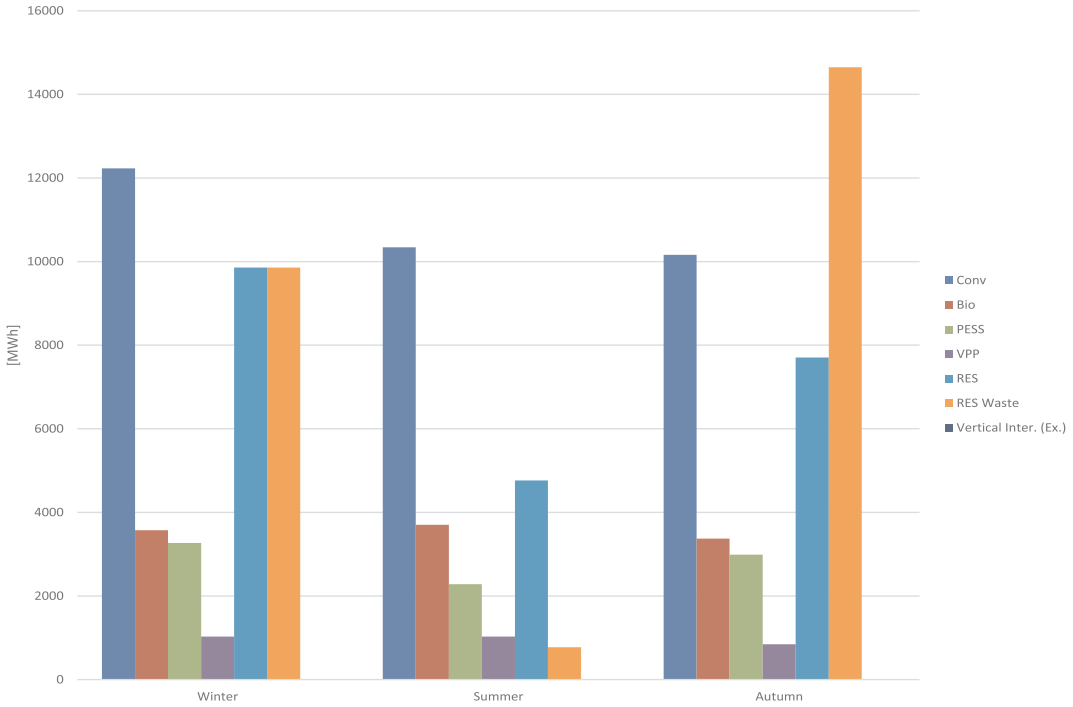

Fig. 26. VPP Case.

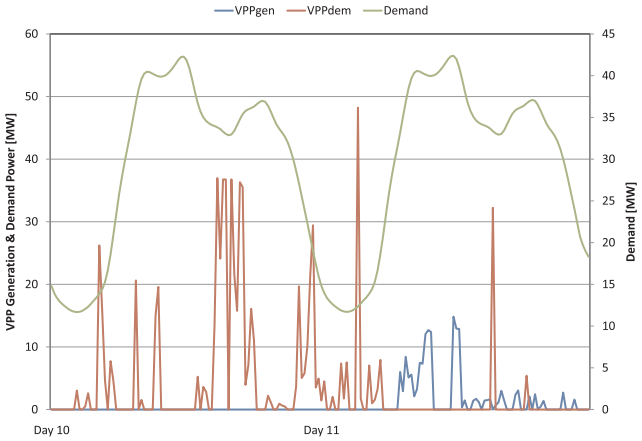

Fig. 27. VPP Summer: Days 10–11.

DSO when the TSO delivers it. Recall that, these energy values are calculated when competing for an "energy-place" in the DSO grid with the other demand-generation resources.

The results for the summer are not surprising because this season has the smallest RES availability. The winter season presents similar values regarding the Export/Import allowance offers. In the autumn season seems to be more advantageous to export energy from the DSO to the TSO. In both seasons, winter and autumn, a clear conclusion arises; DSO-TSO energy exports have a great impact on decreasing RES waste. This fact can be confirmed by the low values on the column RES Waste Export of Table 15.

7. Conclusion

The global energy transition, a shift from conventional to renewable electricity resources, challenges the flexibility of the power grids. In this work, we have developed a methodology that permitted to evaluate the current technological flexibility options available in power grids to exploit the integration of RES fully.

The results demonstrated that, all the flexibility options have the capacity to integrate, in a mayor extent, the RES energy into the power grid. From a base integration of 40.6% of the energy available from RES: PESS option integrated an extra 4.2%, BESS an extra 7.9%, DR an extra 17.9%, VPP an extra 6.9%, and all the flexi-options an extra 27.1% of energy from RES. Thus, the best option to integrate RES is the incorporation of all the flexibility options. The worst option seems to be the PESS expansion, not only on integration figures but also on investment costs. BESS and VPP options seem to have a quite similar impact.

The plausible options (DR and VPP), present the best RES integration figures compared to the onerous options (PESS and BESS); thus, they have the mayor potential for the short-term application. These results, lead us to conclude that it is strongly recommendable to analyze existent options which, with minor modifications, can offer the needed flexibility capacity to proper operation of the power grid.

The results also demonstrated that DSO-DSO energy transactions have a great potential to diminish the RES waste; particularly, in the plausible cases. Compared to the previous base integration of energy from RES (40.6%), DSO-DSO transactions permitted integrating an extra 21.5% for PESS, an extra 14.1% for BESS, an extra 19.7% for DR,

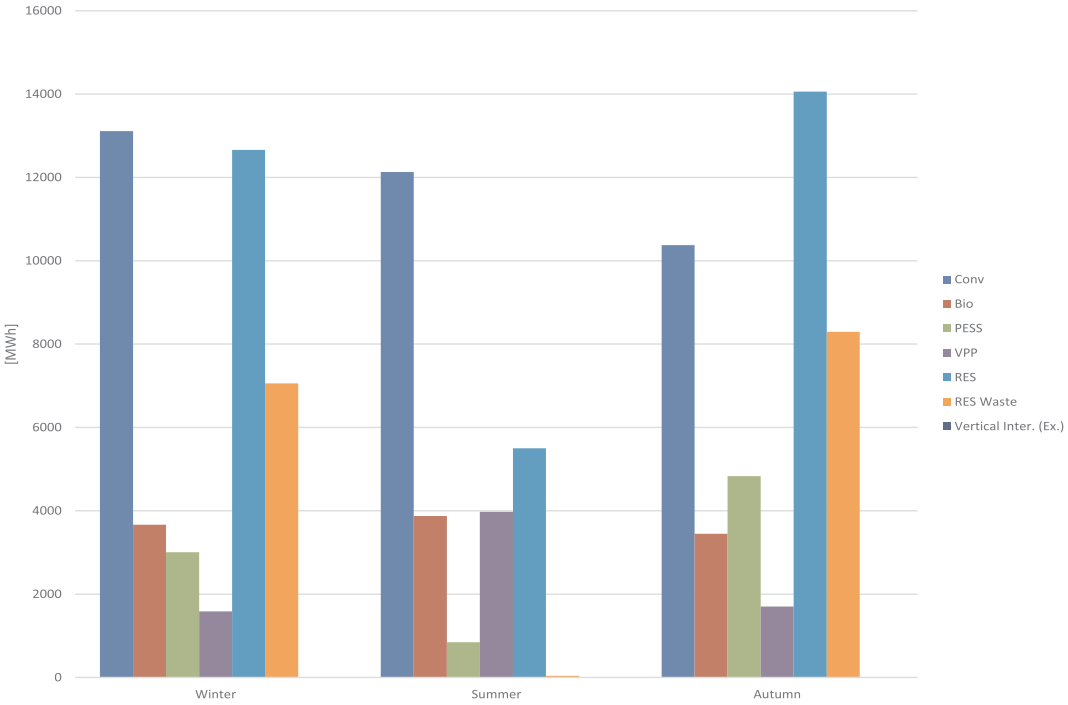

Fig. 28. Full Case.

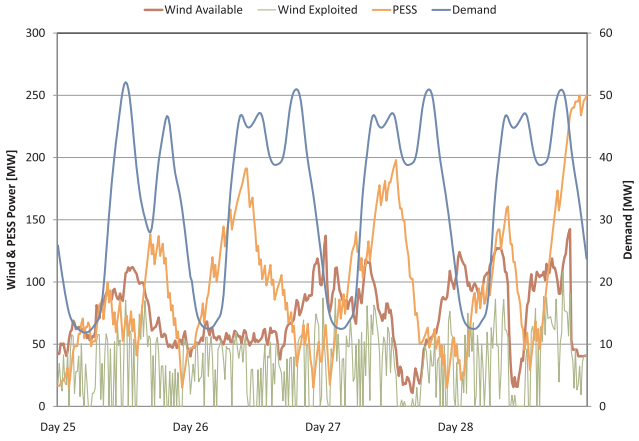

Fig. 29. Full Winter: Days 17–19.

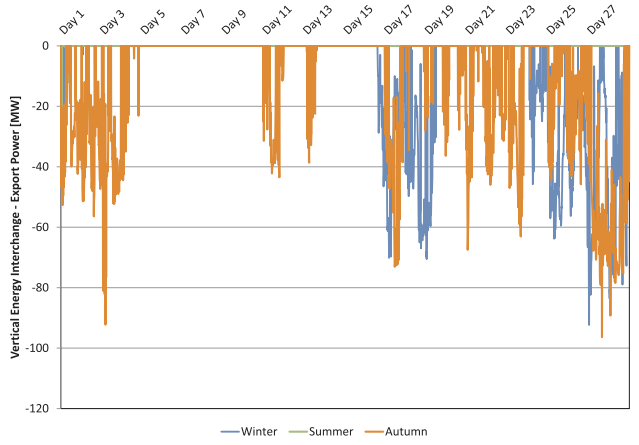

Fig. 30. DSO-TSO export allowance pattern.

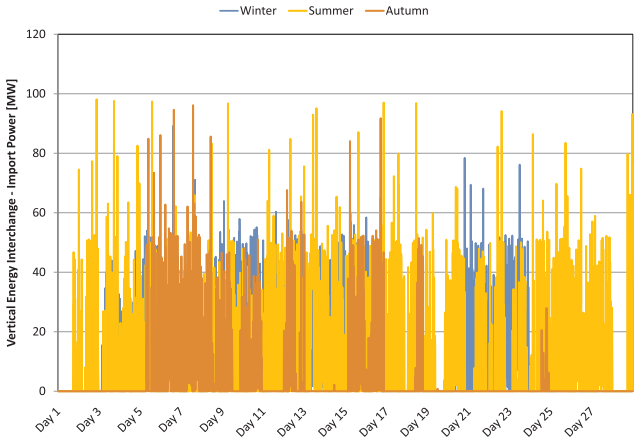

Fig. 31. DSO-TSO import allowance pattern.

Table A.18
BESS Case.

	Total Generation				RES	Vertical	
	Conv	Bio	PESS	RES	curtailment	Inter.	
Season	[MWh]					Im.	Ex.
Winter	12705	3520	3972	9166	10550	–	14.5
Summer	10757	3576	2982	4835	703	–	–
Autumn	10743	3363	5407	8799	13556	–	–

Table A.19
DR Case.

	Total Generation				RES	Vertical
	Conv	Bio	PESS	RES	Curtailment	Inter.
Season	[MWh]					Im./Ex.
Winter	14,757	3590	2428	10,746	8969	–
Summer	15,776	3822	712	5208	329	–
Autumn	12,328	3450	2900	11,875	10480	–

Table A.20
VPP Case.

	Total generation					RES	Vertical
	Conv	Bio	PESS	VPP	RES	Curtailment	Inter.
Season	[MWh]						Exp.
Winter	12,232	3573	3270	1028	9859	9856	4.5
Summer	10,341	3701	2282	1029	4762	776	0.5
Autumn	10,163	3374	2988	847	7705	14650	5.3

Table A.21
Full Case.

	Total Generation					RES	Vertical
	Conv	Bio	PESS	VPP	RES	curtailment	Inter.
Season	[MWh]						Im./Ex.
Winter	13,112	3665	3004	1583	12,659	7057	–
Summer	12,130	3874	845	3976	5498	40	–
Autumn	10,373	3446	4831	1701	14,061	8294	–

an extra 20.6% for VPP, and an extra 13.9% for the full flexi-option. On the other hand, DSO-TSO energy transactions have also a great impact on RES energy integration. For example, energy exports (from the DSO to the TSO) for the full flexi-option permitted integrating RES up to 89.3% in winter, 100% in summer, and 91.3% in autumn. These horizontal-vertical transactions lead us to conclude that, re-engineered electricity markets to cope with extended transactions will be needed, as soon as possible, in the modern power systems with high penetration of RES.

In general, we can conclude that the methodology has the potential to help -market operators/agents, planning/consulting agencies, electricity companies, or governmental agencies/administrators-analyzing different strategies to maximize the integration of RES resources into the grid. This in turn can help to make adequate investment decisions in new grid-flexibility-options deployment.

Acknowledgment

This work is part of the REGEES project, which is funded by the German Federal Ministry for Economic Affairs and Energy under the project number 0325779A. Dr. Alemany gratefully acknowledges financial support from the UNRC and CONICET Argentina, and the Alexander von Humboldt Stiftung, Germany.

Appendix A. Detailed Results for Sections 6.1–6.6

Figs. 26–31.
Tables A.18, A.19, A.20, A.21.

References

[1] 50Hertz Transmission GmbH. <http://www.50hertz.com/en/Grid-Data/Wind-power>.
[2] Fraunhofer ISE – Energy Charts. <https://www.energy-charts.de/index.htm>.
[3] Fraunhofer ISE – Energy Charts. <https://www.energy-charts.de/ren_share.htm?year=all&source=wind-share&period=annual>.
[4] The Federal Ministry for Economic Affairs and Energy, Public Relations, Fifth 'Energy Transition' Monitoring Report, The Energy of the Future, 2015 Reporting Year – Summary, BMWi, Berlin; Dec. 2016. p. 34.
[5] Komarnicki P. Energy storage systems: power grid and energy market use cases. Arch Electr Eng 2017;65:495–511.
[6] Lund P, Lindgren J, Mikkola J, Salpakari J. Review of energy system flexibility measures to enable high levels of variable renewable electricity. Renew Sustain Energy Rev 2015;45:785–807.
[7] Kondziella H, Bruckner T. Flexibility requirements of renewable energy based electricity systems – a review of research results and methodologies. Renew Sustain Energy Rev 2016;53:10–22.
[8] Papaefthymiou G, Dragoon K. Towards 100% renewable energy systems: uncapping power system flexibility. Energy Policy 2016;92:69–82.
[9] Alizadeh M, Moghaddam M, Amjady N, Siano P, Sheikh-El-Eslami M. Flexibility in future power systems with high renewable penetration: a review. Renew Sustain Energy Rev 2016;57:1186–93.
[10] Frew B, Becker S, Dvorak M, Andresen G, Jacobson M. Flexibility mechanisms and pathways to a highly renewable US electricity future. Energy 2016;101:65–78.
[11] Despres J, Mima S, Kitous A, Criqui P, Hadjsaid N, Noirot I. Storage as a flexibility option in power systems with high shares of variable renewable energy sources: a POLES-based analysis. Energy Econ 2017;64:638–50.
[12] Saez A, Martinez E, Stroe D, Swierczynski M, Rodriguez P. Sizing study of second life Li-ion batteries for enhancing renewable energy grid integration. In: IEEE transactions on industry applications Nov.–Dec. 2016;52(6): p. 4999–5008.
[13] McPherson M, Tahseen S. Deploying storage assets to facilitate variable renewable energy integration: the impacts of grid flexibility, renewable penetration, and market structure. Energy 2018;145:856–70.
[14] Krajacic G, Duic N, Carvalho M. How to achieve a 100% RES electricity supply for Portugal? Appl Energy 2011;88:508–17.
[15] Segurado R, Krajacic G, Duic N, Alves L. Increasing the penetration of renewable energy resources in S. Vicente, Cape Verde. Appl Energy 2011;88:466–72.
[16] Xydis G. Comparison study between a Renewable Energy Supply System and a supergrid for achieving 100% from renewable energy sources in Islands. Int J Electr Power Energy Syst 2013;46:198–210.
[17] Gils H. Assessment of the theoretical demand response potential in Europe. Energy 2014;67:1–18.
[18] Neves D, Pina A, Silva C. Demand response modeling: a comparison between tools. Appl Energy 2015;146:288–97.
[19] Welsch M, Deane P, Howells M, Gallachir B, Rogan F, Bazilian M, et al. Incorporating flexibility requirements into long-term energy system models a case study on high levels of renewable electricity penetration in Ireland. Appl Energy 2014;135:600–15.
[20] Belderbos A, Delarue E. Accounting for flexibility in power system planning with renewables. Int J Electr Power Energy Syst 2015;71:33–41.
[21] Thakurta P, Maeght J, Belmans R, Van Hertem D. Increasing transmission grid flexibility by TSO coordination to integrate more wind energy sources while maintaining system security. In: IEEE transactions on sustainable energy Jul. 2015;6(3): 1122–30.
[22] Pavic I, Capuder T, Kuzle I. Low carbon technologies as providers of operational flexibility in future power systems. Appl Energy 2016;168:724–38.
[23] Krakowski V, Assoumou E, Mazauric V, Maizi N. Feasible path toward 40100% renewable energy shares for power supply in France by 2050: a prospective analysis. Appl Energy 2016;171:501–22.
[24] Hirth L. The benefits of flexibility: the value of wind energy with hydropower. Appl Energy 2016;181:210–23.
[25] Lombardi P, Sokolnikova T, Suslov K, Voropai N, Styczynski ZA. Isolated power system in Russia: a chance for renewable energies? Renew Energy 2016;90:532–41.
[26] Zou P, Chen Q, Yu Y, Xia Q, Kang C. Electricity markets evolution with the changing generation mix: an empirical analysis based on China 2050 High Renewable Energy Penetration Roadmap. Appl Energy 2017;185(Part 1): 56–67.
[27] Lombardi P, Schwabe F. Sharing economy as a new business model for energy storage systems. Appl Energy 2017;188:485–96.
[28] Alemany J, Magnago F, Lombardi P, Arendarski B, Komarnicki P. Multiobjective optimization model for wind power allocation, mathematical problems in engineering; 2017.
[29] Wood A, Wollenberg B, Shebl G. Power generation, operation, and control. 3rd ed. Wiley; 2013. 656.
[30] Nowak M, Rmisch W. Stochastic Lagrangian relaxation applied to power scheduling in a hydro-thermal system under uncertainty. Annals Oper Res 2000;100(14):251272.
[31] Fox B et. al. Wind power integration: connection and system operational aspects, Institution of Engineering and Technology, Science; Jun. 2013. p. 318.
[32] Stott B, Jardim J, Alsac O. DC power flow revisited. In: IEEE transactions on power systems Aug. 2009;24(3): 1290–300.
[33] Purchala K, Meeus L, Van Dommelen D, Belmans R. Usefulness of DC power flow for active power flow analysis. In: Proc IEEE PES general meeting, San Francisco, CA, USA; Jun. 2005.
[34] Akbari T, Tavakoli Bina M. Linear approximated formulation of AC optimal power flow using binary discretisation. IET Gener, Transmiss Distribut Jul. 2016;10:1117–23.
[35] Pandzic H, Wang Y, Qiu T, Dvorkin Y, Kirschen D. Near-optimal method for siting and sizing of distributed storage in a transmission network. IEEE Trans Power Syst Sept. 2015;30(5): 2288–300.
[36] Magnago F, Alemany J, Lin J. Impact of demand response resources on unit commitment and dispatch in a day-ahead electricity market. Int J Electr Power Energy Syst 2015;68:142–9.
[37] Morales J et. al. Integrating renewables in electricity markets. International Series in Operations Research & Management Science 205, Springer; 2014.
[38] Fahd G, Richards D, Sheble G. The implementation of an energy brokerage system using linear programming. IEEE Trans Power Syst Feb. 1992;7(1): 90–96.
[39] Fraunhofer ISE - Energy Charts. <https://www.energy-charts.de/osm.htm>.
[40] Bradley S, Hax A, Magnanti T. Applied mathematical programming, Addison-Wesley; 1977.
[41] 50Hertz Transmission GmbH. <http://www.50hertz.com/en/>.